AFML-TR-78-178

LEVEL

RESEARCH ON INHIBITION FOR CORROSION FATIGUE OF HIGH STRENGTH ALLOYS

UNIVERSITY OF FLORIDA
GAINESVILLE, FLORIDA 32611

BOEING AEROSPACE CORPORATION
SEATTLE, WASHINGTON 98124

15 DECEMBER 1978

TECHNICAL REPORT AFFDL-TR-76-137
Final Report for Period 15 May 1975 to 2 October 1978

Approved for public release; distribution unlimited.

OFFICE OF NAVAL RESEARCH RESIDENT REPRESENTATIVE
GEORGIA INSTITUTE OF TECHNOLOGY
ATLANTA, GEORGIA 30332

AIR FORCE MATERIALS LABORATORY
AIR FORCE WRIGHT AERONAUTICAL LABORATORIES
AIR FORCE SYSTEMS COMMAND
WRIGHT-PATTERSON AIR FORCE BASE, OHIO 45433

NOTICE

When Government drawings, specifications, or other data are used for any purpose other than in connection with a definitely related Government procurement operation, the United States Government thereby incurs no responsibility nor any obligation whatsoever; and the fact that the government may have formulated, furnished, or in any way supplied the said drawings, specifications, or other data, is not to be regarded by implication or otherwise as in any manner licensing the holder or any other person or corporation, or conveying any rights or permission to manufacture, use, or sell any patented invention that may in any way be related thereto.

This report has been reviewed by the Information Office (OI) and is releasable to the National Technical Information Service (NTIS). At NTIS, it will be available to the general public, including foreign nations.

This technical report has been reviewed and is approved for publication.

Charles T. Lynch

PROJECT ENGINEER
METALS BEHAVIOR BRANCH
METALS AND CERAMICS DIVISION

N G Tupper

NATHAN G. TUPPER, Chief
METALS BEHAVIOR BRANCH
METALS AND CERAMICS DIVISION

"If your address has changed, if you wish to be removed from our mailing list, or if the addressee is no longer employed by your organization please notify AFML/LLN ,W-PAFB, OH 45433 to help us maintain a current mailing list".

Copies of this report should not be returned unless return is required by security considerations, contractual obligations, or notice on a specific document.

SECURITY CLASSIFICATION OF THIS PAGE (When Data Entered)

REPORT DOCUMENTATION PAGE		READ INSTRUCTIONS BEFORE COMPLETING FORM
1. REPORT NUMBER AFML-TR-78-178	2. GOVT ACCESSION NO.	3. RECIPIENT'S CATALOG NUMBER
4. TITLE (and Subtitle) RESEARCH ON INHIBITION FOR CORROSION FATIGUE OF HIGH STRENGTH ALLOYS		5. TYPE OF REPORT & PERIOD COVERED Final Report, 15 May 1975 - 2 October 1978
		6. PERFORMING ORG. REPORT NUMBER
7. AUTHOR(s) Ellis D. Verink, Jr. K. Bhagwan Das		8. CONTRACT OR GRANT NUMBER(s) F33615-75-C-5200
9. PERFORMING ORGANIZATION NAME AND ADDRESS University of Florida, Engineering and Industrial Experiment Station, Gainesville, FL 32611 and Boeing Aerospace Group, P.O. Box 3999, Seattle, WA 98124		10. PROGRAM ELEMENT, PROJECT, TASK AREA & WORK UNIT NUMBERS Project # - 2306 Task # - 2306 P6 Work Unit # - 2306 P6 01
11. CONTROLLING OFFICE NAME AND ADDRESS Air Force Materials Laboratory (LLN) Wright-Patterson AFB, Ohio 45433		12. REPORT DATE 15 December 1978
		13. NUMBER OF PAGES 101 pages
14. MONITORING AGENCY NAME & ADDRESS (if different from Controlling Office) Office of Naval Research Resident Representative Georgia Institute of Technology 325 Hinman Research Building Atlanta, Georgia 30332		15. SECURITY CLASS. (of this report) Unclassified
		15a. DECLASSIFICATION/DOWNGRADING SCHEDULE

16. DISTRIBUTION STATEMENT (of this Report)

Approved for public release, distribution unlimited.

17. DISTRIBUTION STATEMENT (of the abstract entered in Block 20, if different from Report)

18. SUPPLEMENTARY NOTES

19. KEY WORDS (Continue on reverse side if necessary and identify by block number)

Inhibitors, hydrogen embrittlement, stress corrosion, fracture toughness testing, polarization resistance, crevice corrosion, hydrogen analysis, high strength steels.

20. ABSTRACT (Continue on reverse side if necessary and identify by block number)

Over 200 potential inhibitor compositions were screened in selecting three final candidates to test in determining the effectiveness of oxidizing inhibitors in controlling hydrogen embrittlement of aerospace structural materials. Alloys tested included 4340, 300M, 17-4 PH, HP 9-4-30 and HY180. The three final inhibitors were the "blocking type" inhibitors, piperidine, and piperazine and a proprietary, polyfunctional inhibitor Nalco 39L. When present in sufficient concentration (1 M), the blocking inhibitors reduced hydrogen content at (or near) the fracture surface significantly, reduced the

over

DD FORM 1473, 1 JAN 73 EDITION OF 1 NOV 65 IS OBSOLETE

SECURITY CLASSIFICATION OF THIS PAGE (When Data Entered)

408 174

79 04 12 038

SUB ISCC

Block 20 SUB IC

crack growth rate several orders of magnitude and increased K_{Iscc} to approximately K_{Ic} under static conditions. The polyfunctional inhibitor reduced measured hydrogen content to the lowest levels (of the three inhibitors), however, only the manufacturer's recommended concentration was generally effective. At lower as well as higher concentrations crack growth rates increased. At low concentrations, the fracture character resembled hydrogen embrittlement whereas at higher concentrations active path cracking was observed. Suggestions are made for future research.

FOREWORD

This report was prepared jointly by Dr. Ellis D. Verink, Jr., of University of Florida, and Dr. K. B. Das, of the Boeing Company under AFML Contract #F33615-75-C-5200-1 entitled "Research on Inhibitors for Corrosion Fatigue of High Strength Alloys." Project Scientist monitoring this program was Dr. C. T. Lynch of AFML/LLN.

This report covers work performed during the period from 15 May 1975 to 1 October 1978 and was submitted by the authors 1 October 1978.

This program was conducted jointly by the Department of Materials Science and Engineering of the University of Florida, Gainesville, Florida under the supervision of Dr. Ellis D. Verink, Jr., and the Boeing Aircraft Company under the supervision of Dr. K. B. Das. Electrochemical studies, inhibitor screening tests and certain fracture toughness tests were performed at University of Florida. Initial characterization of the starting materials plus fracture toughness experiments and the hydrogen analyses of fracture surfaces were performed by the Research and Engineering Division of the Boeing Aerospace Company, Seattle, Washington. The project provided at least partial support for several graduate students at the University of Florida.

TABLE OF CONTENTS

LIST OF FIGURES

LIST OF TABLES

SECTION 1

INTRODUCTION

Earlier work at the University of Florida under Air Force Contract F33615-73-C-5007 as well as work at the Air Force Materials Laboratories showed that oxidizing inhibitors are capable of retarding crack growth in certain high strength alloy steels subjected to aqueous solution. Particular reference is made to the work of Parrish,[1,2] and Johnson[3] who studied the influence of inhibitors on "crevice corrosion" behavior of D6AC alloy in saline solutions. Johnson observed the phenomenon of a "crevice protection potential." At electrode potentials more noble than this potential, acidification and intensification of corrosion occurred within crevices. At potentials more active than the crevice protection potential, corrosion within crevices ceased and the crevice pH became more alkaline. These observations are important since acidification within a crevice can lead to entry of hydrogen into steel. As also reported by others,[3,4] the electrode potentials within an active pit, crevice or propagating crack,[5] can be below (more active than) the equilibrium hydrogen solution potential (because of local acidification) despite the fact that the bulk pH may be much more alkaline. Another key observation was that oxidizing inhibitors may be used to control the electrochemical processes within occluded cells and thus to prevent crevice corrosion. Parrish[1] extended this work to show a correlation between the effectiveness of oxidizing inhibitors in preventing crevice corrosion with the amount and distribution of hydrogen in D6AC steel fracture toughness specimens. He illustrated the effect by using chromate solutions and hydrazine solutions to illustrate the possibility of increasing K_{Iscc} and reducing crack velocity by use of oxidizing inhibitors. The present study extends the work of

Parrish, Johnson and others to a range of alloys of interest to the Air Force. Over two hundred inhibitor compounds and formulations were surveyed with regard to their effect on the electrochemical behavior, fracture toughness behavior, and influence on hydrogen content of alloys 4340, 300M, 17-4 PH and HP 9-4-30. At a later stage of the investigation, alloy HY180 was supplied for partial examination and some data are also submitted on this material. While a number of quite specific conclusions were made possible as a result of this research, there are a number of avenues of future research which should prove productive. These are ennumerated at the end of the report.

SECTION 2

GENERAL BACKCROUND AND OBJECTIVE OF THE PROGRAM

High strength steels such as D6AC, 4340, 300M, etc., have shown a decided tendency to fail under stress by hydrogen embrittlement.[6-8] The development of a practical method of preventing hydrogen entry into these steels would be of immense engineering value. These alloys could then presumably be used either at higher strength levels or with assurance at present strength levels. Parrish showed that hydrazine was able to reduce crack growth rate by about an order of magnitude even in 0.1 M sodium chloride solution. Furthermore, 2% by weight of hydrazine added to the electrolyte increased K_{Iscc} from 12 to 25 ksi $\sqrt{\text{inches}}$. Such an increase in K_{Iscc} is important since the critical flaw size varies as $(K_{Iscc})^2$ and an increase in critical flaw size makes more likely the nondestructive detection of critical size flaws.

In the hydrazine inhibition mechanism, NO_2^- is formed. This in turn controls the crack tip electrode potential and pH so that hydrogen evolution in the crack is prevented and a passive γFe_2O_3 film is formed. The ultrasensitive hydrogen detector of Das[9] was used to determine the hydrogen concentration on (and near) the fracture surface. The results confirmed that the inhibitor prevented hydrogen entry at the crack tip. Unfortunately, hydrazine is an inconvenient material for general usage, however, the results suggested that the direct use of nitrite-containing-compounds instead of hydrazine may be appropriate. Preliminary experiments with sodium nitrite indicated that it was at least as effective as hydrazine in lowering the crack growth rates for D6AC steel.

Aircraft parts made of high strength steels normally receive a mechanical treatment such as shot-peening to leave the surface in a net compressive state of stress. Steel parts are then cadmium plated, given an epoxy primer and a polyurethane topcoat. When inhibitors are incorporated, this is normally done in a primer coat. One of the most important considerations in the selection of an inhibitor is compatibility with the epoxy (or other primer) in combination with an ability to inhibit or prevent corrosion (either general corrosion or localized types of corrosion such as stress corrosion cracking, pitting, etc.). Zinc chromate formulations have been most widely used. Water soluble inhibitors (such as chromates) provide mobility in the inhibitor function. Unfortunately, chromates are toxic so care must be exercised in their use. In addition, as shown by Parrish,[1,2] in the presence of chlorides, chromates are not effective in preventing hydrogen embrittlement of D6AC.

Commerical inhibitor formulations such as those used for cooling tower circuits, automotive radiators, and so forth, normally are combinations of several classes of inhibitor compounds some of which function as anodic inhibitors, others as cathodic inhibitors. Commerical experience has shown that such combinations often are more effective than inhibitors used separately. In short, there seems to be evidence for "synergism."[10] Accordingly, tests were conducted[11] using a borax-nitrite-polyphosphate commercial formulation (Calgon) in combination with chromate systems. Results from crack growth measurements on D6AC in distilled water containing the multifunctional inhibitor showed that the crack growth rate was reduced by 1/2 an order of magnitude and that K_{Iscc} was increased from 77 to 82 ksi $\sqrt{\text{inches}}$ as compared to inhibited formulations containing only chromates. This promising result from multifunctional inhibitors was observed both in static tests and in cyclic corrosion fatigue tests. This observation has led to the field testing of multifunctional inhibitors in wash racks for aircraft by the Air Force.

The highly encouraging results with D6AC steel led naturally to an interest in determining whether similar salutary effects could be achieved by use of inhibitors with other alloys of aerospace interest, notably 4340, 300M, HY180, 17-4 PH and HP 9-4-30.

SECTION 3

EXPERIMENTAL

A research program was undertaken to try to find if there were an inhibitor (or perhaps a small group of inhibitors) which would function favorably for all of the above mentioned alloys.

The research was divided into several functional phases. Phase I included the chemical and electrochemical-mechanical characterization of the candidate alloys. Characterization also included the establishment of "base-line" values for initial hydrogen content. Concurrently with the conduct of Phase I, specimens for fracture toughness experiments for use in Phase III were machined, precracked and stored.

Phase II consisted of selecting promising inhibitor candidates from the generic types shown in Table 1 and screening the list down to a few for detailed testing. Over two hundred candidate materials were considered.

Phase III took the output of Phases I and II and applied the results to compact tension fracture toughness specimens. The influence of the selected inhibitor was assessed in terms of its influence on K_{Iscc}, crack growth rate and (final) hydrogen content at and near the fracture surface.

It was quickly evident as the screening process was undertaken that there would be considerable advantage to having better, more scientifically based methods of screening inhibitors. As a consequence, a subordinate effort was carried on concurrently with this program in an effort to determine whether other methods might hold promise for future research.

TABLE 1

INHIBITORS - COMPOUNDS

CATHODIC	Polyphosphate Zinc Silicate
ANODIC	Orthophosphate Chromate Ferrocyanide Nitrite
COMBINATIONS	Polyphosphate-Chromate Polyphosphate-Ferrocyanide Borax-Nitrite Fluoride-Chromate Benzoate-Nitrite Silicate-Chromate
FILM FORMERS	Emulsified or Soluble Oils Octadecylamine Long Chain Amines Alcohols and Carboxylic Acids

TABLE 2

CHEMICAL COMPOSITION

Alloy	C	Mn	P	S	Si	Cr	Ni	Cu	Mo	Co
17-4 PH	0.036	0.49	0.022	0.016	0.63	15.69	4.32	3.50	--	--
HP 9-4-30*	0.310	0.29	0.001	0.007	0.06	1.10	7.88	0.28	1.08	4.50
4340	0.42	0.72	0.010	0.012	0.32	0.77	1.84	0.13	0.22	--
HY180	0.14	0.14	--	--	0.09	2.0	10.0	--	1.2	14.4

*HP 9-4-30 -- Consumable Electrode Vacuum Melted

TABLE 3

MECHANICAL PROPERTIES OF COMPACT TENSION SPECIMENS

Alloy	Yield Strength (psi)	Ultimate Tensile Strength (psi)	Percent Elongation	Hardness
17-4 PH	185,000	200,000	5	R_c4
HP 9-4-30	207,800	246,000	15	R_c4
4340	210,000	256,100	1	R_c56
HY180	229,000	250,000	15.5	R_c49

TABLE 4: HYDROGEN ANALYSIS

Trial #	Material / Hydrogen Content	4340 Steel 1" Plate (ppm)	300M Steel 1" x 2" Bar (ppm)	17-4 PH Steel 1" Plate (ppm)	HP 9-4-30 Steel 1" Plate (ppm)	4340 Steel Sheet (ppm)	300M Steel Sheet (ppm)	17-4 PH Steel Sheet (ppm)	HP 9-4-30 Steel Sheet (ppm)	HY180 Steel Sheet (ppm)
1	H_1	3.67	2.33	2.35	1.13	1.77	3.45	3.24	1.13	0.87
2	H_2	3.31	1.65	1.81	1.23	1.45	3.63	2.81	1.23	0.60
3	H_3	3.50	2.85	1.94	0.75	2.19	3.72	3.53	0.75	0.60
4	H_4	3.56	2.67	2.56	0.94	1.93	3.22	3.53	0.94	0.53
5	H_5	3.29	1.62	1.70	1.37	1.70	2.81	2.96	1.37	0.94
6	H_6	2.41	2.78	1.89	0.78	1.79	3.36	2.95	0.78	0.65
# of Determinations - n		6	6	6	6	6	6	6	6	6
Mean - $\bar{c}$		3.29	2.32	2.04	1.03	1.81	3.37	3.17	1.03	0.70
Std. Dev. - σ		.4552	.5568	.3369	.2508	.2459	.3264	.3118	.2508	.1777
Coeff. of Variance - $(\sigma/\bar{c})$ %		13.84	24.00	16.51	24.35	13.59	9.69	9.84	24.35	25.39
Std. Error - $\sigma/\sqrt{n}$		.1858	.2273	.1375	.1024	.1004	.1333	.1273	0.10	.0725
95% Confidence Limits - $E_{\bar{c}} = (t\sigma)/\sqrt{n}$		±.4778	±.5844	±.3536	±.2633	±.2582	±.3426	±.3273	±.2633	±.1865
Fractional Random Error in Mean - $(E_{\bar{c}}/\bar{c})$		14.50	25.19	17.33	25.56	14.26	10.17	10.32	25.56	26.65

SECTION 3.1

PHASE I - CHARACTERIZATION OF TEST MATERIALS

The chemical compositions of the alloys used in the experimental program are given in Table 2. Mechanical properties of these alloys are given in Table 3. The details of heat treatment are given in Appendix 1. The initial hydrogen contents of the materials are given in Table 4. A description of the ultra-sensitive hydrogen detector of Das is included in Appendix 2. The characterization process involved electrochemical potentiokinetic characterization in the form of polarization curves and potential versus pH diagrams for each of the alloys in 0.1 N chloride solutions at room temperature. As indicated above, each of the alloys was characterized as to initial (base-line) hydrogen content. At the completion of fracture toughness experiments, the samples were re-analyzed for hydrogen content at (or near) the fracture surface. Reaction product films were analyzed by x-ray analysis and/or Auger electron spectroscopy as appropriate. Potential pH diagrams (Pourbaix diagrams) were calculated for each of the constituents of each of the alloys and are included in Appendix 3. Superposition of the Pourbaix diagram of elements which serve as constituents of individual alloys often can provide useful insights into the interpretation of corrosion behavior. Experimental potential pH diagrams also were developed for each of the alloys and are included in Appendix 3. The apparatus and procedure for the development of such diagrams is reported elsewhere.[12] Studies of occluded cell behavior of these alloys were made using a test cell similar to that developed by Efird.[13] As indicated by Efird, acidification is expected in crevices where the bulk pH is above the "crevice protection potential." In these cases where the final electrode potential and pH within the occluded cell falls below the equilibrium hydrogen line, hydrogen charging is expected. Crevice experiments with each of the alloys (4340, 300M, HY180, 17-4 PH and HP 9-4-30) showed acidification within crevices.

SECTION 3.2

PHASE II - SELECTION OF INHIBITOR CANDIDATES

3.2.1. Crevice Tests - The screening of inhibitors of the types listed in Table 1 proved to be a complex process and the strategy for accomplishing the screening process required some revision as the research progressed. The first step of the screening process involved the question of toxicity. If an inhibitor species was obviously toxic based on literature information[14] it was eliminated from further consideration for this reason. Chromates, aniline and arsenic additions are examples of inhibitors which were eliminated on this basis. On the other hand, it was necessary to exercise some restraint since to eliminate all materials which might conceivably be toxic under some special circumstances could eliminate almost everything. Since specific guidelines on toxicity were not available, qualitative judgments were used in the assessment of relative toxicity. Figure 1 shows a montage of types of specimen configurations used in various portions of the research program. The first series of tests involved the formation of an artificial crevice made up of two metal pieces joined mechanically with the use of a plastic screw and nut, Figure 2. These assemblies were exposed in plastic bottles in acidic, neutral and alkaline solutions with chlorides present, Figure 3. Parallel samples of each test alloy were exposed in each electrolyte with and without inhibitor additions. The inhibitor concentration followed the manufacturer's recommendation (if

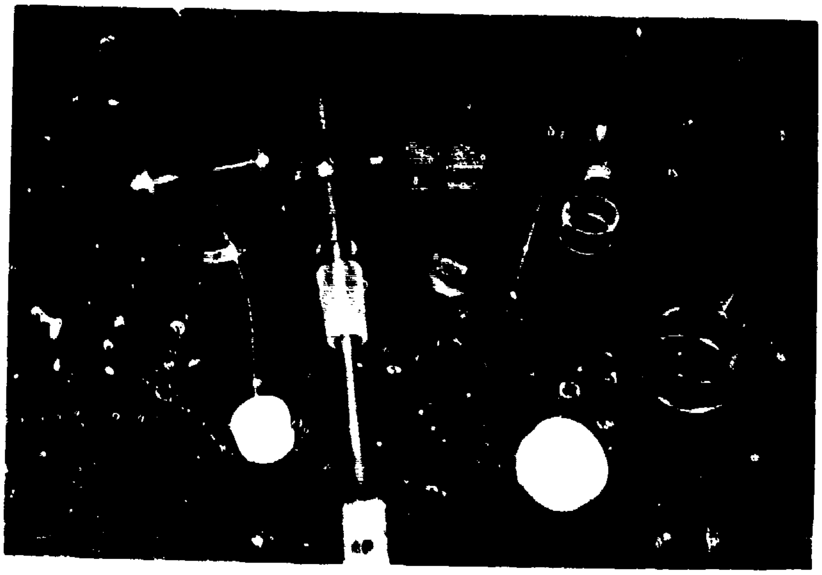

Figure 1. Configurations of test specimens employed in screening and testing of effectiveness of inhibitor candidates.

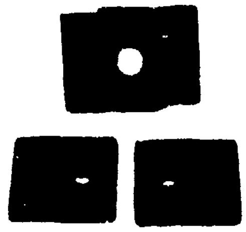

Figure 2. Artificial crevice samples made of two sheet samples joined with a plastic bolt and nut. These samples were exposed in plastic bottles containing inhibited chloride solutions, Figure 3.

Figure 3. Specimens (see Figure 2) were exposed to uninhibited and inhibited chloride solutions as part of the screening process. Candidate inhibitors which caused crevice corrosion were eliminated at this stage.

there was one), or was selected from information in the corrosion literature. A third level also was employed, this being one tenth the recommended concentration level. Evaluation of these samples was by visual examination to see whether or not crevice corrosion occurred. Inhibitor formulations which stimulated crevice corrosion were dropped without further tests. It was observed that the inhibitor effect varied with pH in a number of cases. For example, 4340 alloy in acidic solutions containing 0.1 N sodium silicate suffered crevice corrosion and pitting in 7 days whereas in alkaline solutions of pH 12.9 this level of inhibitor appeared to be completely protective after 24 days. In neutral solution, the changes were primarily in visual appearance (local darkening, etc.). Specimens of HP 9-4-30 in neutral and alkaline solutions containing 0.1 N sodium nitrite were free of pitting and crevice corrosion. Several samples were selected for Auger spectrographic analysis of surface films. It soon became obvious that time would not permit an initial screening of each of the nearly 200 inhibitor formulations using bolted crevice assemblies, so a revised procedure for initial screening was devised to improve productivity. This led to the development of the so-called dip test.

3.2.2. Dip Test - One of the goals of this research was to select inhibitors would reduce the danger of hydrogen embrittlement of the test alloys. As indicated above, in crevices and other occluded cells, hydrogen charging of the specimens attended the acidification which occurs. Therefore, in order to combat the tendency for hydrogen charging (and hence avoid hydrogen embrittlement), it was postulated that a potentially useful inhibitor should cause the electrode potential of the alloy to become more noble, or the pH of the electrolyte should

Figure 4. Test apparatus for the "dip test." The influence on pH, electrode potential and current of progressively larger additions of inhibitors to chloride solutions was determined for candidate alloys. Refer to Table 6.

increase upon addition of the inhibitor, or both. In the dip test, specimens (5/8" x 1/2") of each of the four alloys were mounted in metallographic mounting material (cold mount) after soldering an electrical contact to the back of each specimen. Specimens then were polished through a series of grits starting with 240 and finishing with 600 grit silicon carbide. Polished specimens then were carefully cleaned with the following cleaning procedure:

1. Rinse with tap water.
2. Wash with Alconox.
3. Rinse with distilled water.
4. Rinse with tetrachloroethane.
5. Wash with distilled water.
6. Rinse with acetone.
7. Blow dry in hot air.

Specimens then were exposed in a test cell shown in Figure 4. The pH of the solution, electrode potential and corrosion current were monitored as a function of time. Specimens were immersed in 500 ml. of oxygen-saturated electrolyte. The duration of each test was determined by how long it took an individual reading to attain "steady-state." Steady-state was assumed when the values of pH, electrode potential or current remained constaint for a period of at least an hour. After establishing a steady-state condition, inhibitors were added to the solutions. Five ml. of a specific concentration of inhibitor were added at a time and the pH, electrode potential and current were allowed to re-equilibrate to new values. The process was then repeated making successive 5 ml. additions until the final concentration was achieved. This process was performed for 63 alloy and inhibitor concentrations and the results are listed in Table 5. These

TABLE 5

RESULTS OF DIP TEST FOR SCREENING OF INHIBITOR CANDIDATES

	No Go	Go
Benzotriazole	*	
Benzimidazole	*	
Pyridine	*	
Piperidine		*
Thioglycolic Acid	*	
Thiosemicarbazide	*	
1 - Butanedthiol	*	
1-3 Propanediamine	*	
2 - Propyn - 1 - ol	*	
Cyclohhexylamine	*	
Cyanoguanidine	*	
Triethylamine	*	
Diamylamine	*	
Triamylamine	*	
Crotonaldehyde	*	
Piperazine		*
Sodium Silicate	*	
Sodium Nitrite	*	
Nalco 39L		*
Nalco 41L	*	

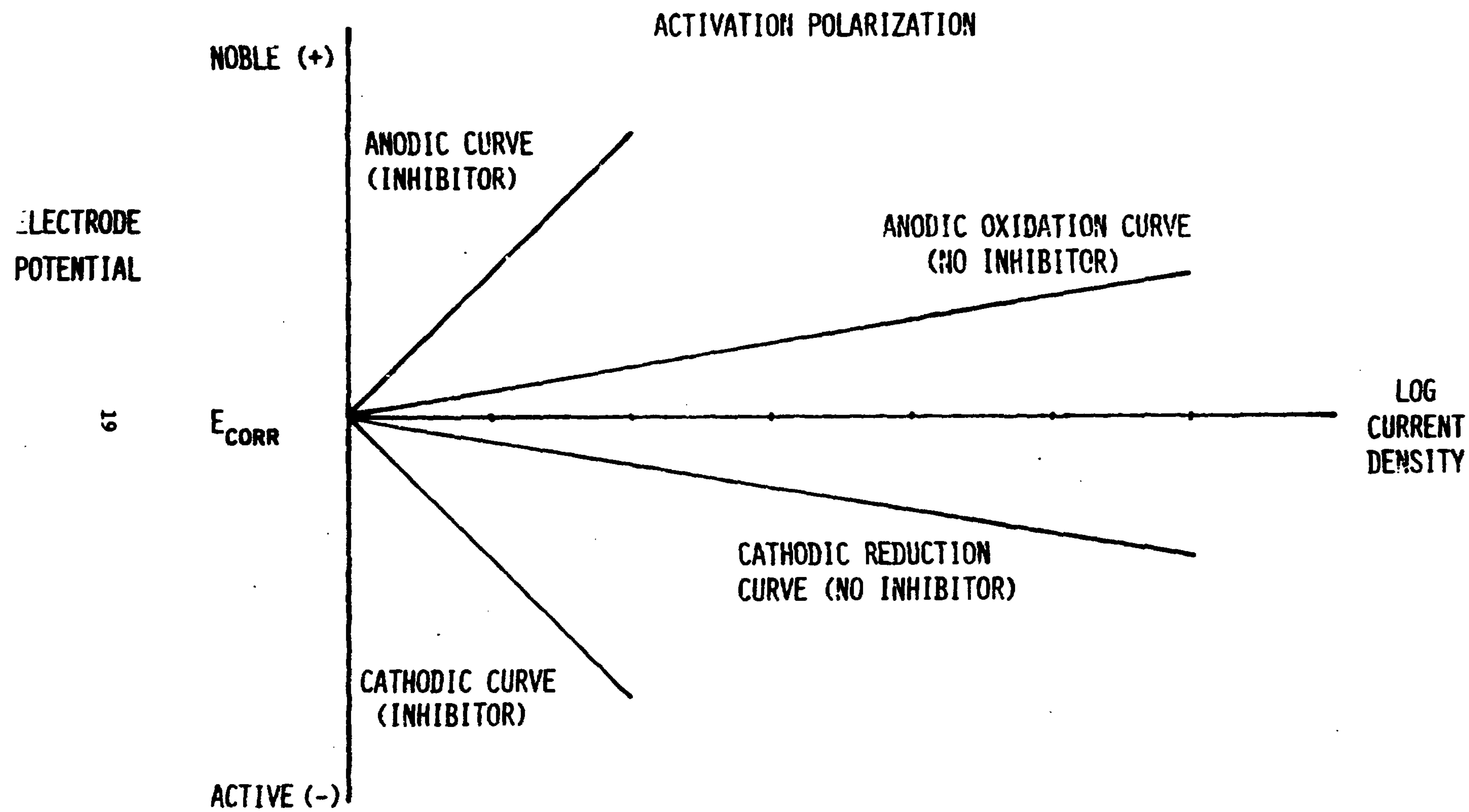

FIGURE 5. SCHEMATIC CATHODIC AND ANODIC POLARIZATION CURVE

are designated as "go" and "no go" depending on whether or not the electrode potential and/or the pH moved in the desired direction. As indicated in Table 5, three inhibitor candidates, piperidine, piperazine and a multifunctional inhibitor, Nalco 39L*, appeared particularly promising. These materials were then subjected to linear polarization tests.

3.2.3. Linear Polarization Tests - Linear polarization tests were for the purpose of verifying whether or not the addition of an inhibitor made a change in the instantaneous corrosion rate. Such tests also provide evidence as to whether or not the effectiveness of the inhibitor is most pronounced at cathodic areas, anodic areas or over both anodic and cathodic areas. Figure 5 shows schematically the influence of inhibitors on the polarization resistance. The greater the change in slope as compared to the uninhibited solution, the more effective the inhibitor. If the change in slope is only on the anodic leg of the curve, the inhibitor is an anodic inhibitor. If the slope is changed only on the cathodic leg, the inhibitor is a cathodic inhibitor and if the slope is increased on both the anodic and cathodic legs, the inhibitor is one which influences the processes at both anodes and cathodes. The equipment for making linear polarization tests is shown in Figure 6. Table 6 summarizes the linear polarization data for the three successful inhibitors for each of the four alloys under consideration. The <u>top entries</u> in each of the groupings show the anodic and cathodic slopes for the alloy <u>without</u> an inhibitor. In each case, the uninhibited solution was acidified to a pH of approximately 3 using hydrochloric acid. This choice is in acknowledgement of the fact that if

*Trade name of Nalco Chemical Company.

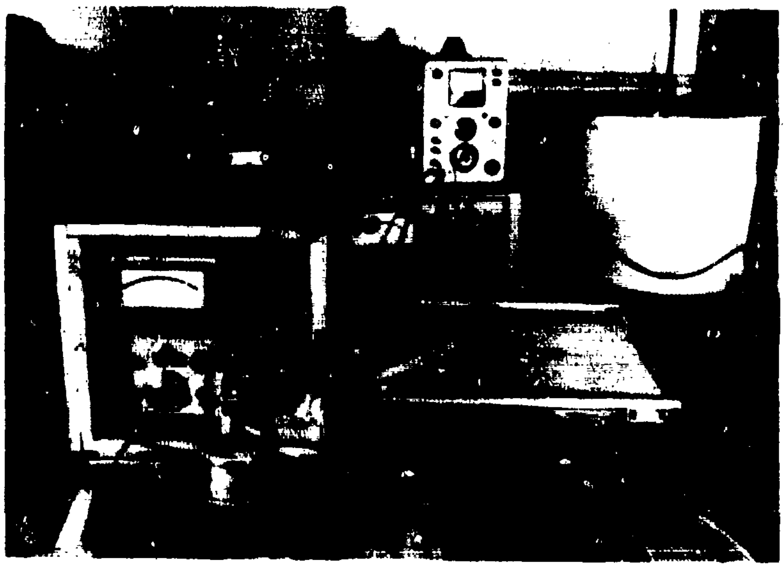

Figure 6. Linear polarization apparatus used to determine "polarization resistance" of candidate materials in various inhibited aqueous chloride solutions at room temperature. See Table 6.

TABLE 6

LINEAR POLARIZATION DATA FROM INHIBITOR SCREENING TESTS

Alloy	Solution		Shapes (E/I)	
	Inhibitor	pH	Anodic	Cathodic
4340	--	3.1	105	105
4340	Nalco 39L	8.1	115	123
4340	Piperidine	5.4	133	133
4340	Piperazine	5.1	123	121
HY180	--	3.1	125	125
HY180	Nalco 39L	3.3	10526	10526
HY180	Piperidine	6.0	10667	11048
HY180	Piperazine	7.0	1333	1333
17-4 PH	--	3.1	7692	7500
17-4 PH	Nalco 39L	3.3	10^{10}	10^{10}
17-4 PH	Piperidine	10.6	12000	11000
17-4 PH	Piperazine	10.1	10526	10526
HP 9-4-30	--	3.1	1090	1077
HP 9-4-30	Nalco 39L	3.3	1710	1880
HP 9-4-30	Piperidine	4.5	10^{10}	10^{10}
HP 9-4-30	Piperazine	6.9	1143	1090

acidification occurs in an occluded cell in the presence of chloride, the pH is likely to be in this regime. Although the specific data showed considerable spread for the various alloys, each of the inhibitors increased the polarization resistance for each of the alloys for both the anodic and cathodic legs of the curve. This indicates that each of these three inhibitors affects both anodic and cathodic processes.

Initially, it was the plan to expose each of the alloys to each of the successful inhibitor concentrations as stressed specimens to assess the cracking propensities as a function of time. Inasmuch as such tests could take a very long time (particularly if the inhibitors were effective) it was decided to abandon this additional screening and proceed directly to testing of compact fracture toughness specimens in electrolytes with and without inhibitors.

SECTION 3.3

PHASE III - FRACTURE TOUGHNESS TESTS AND HYDROGEN ANALYSES

3.3.1. Fracture Toughness Tests - Compact tension specimens of 4340, 300M, 17-4 PH and HP 9-4-30, as shown in Figure 7, were used to determine K_{Iscc} and crack growth rate in various environments. Bolt-loaded specimens were employed in the tests at University of Florida, since their use would minimize equipment required while maximizing the obtaining of useful data, Figure 9. Concurrent K_{Iscc} and crack growth rate studies were conducted at the Boeing Company under the direction of Dr. K. B. Das using a modified creep machine, Figure 10. A close-up of the test arrangement appears as Figure 11. It was satisfying to observe that fracture toughness data from these two different methods of making measurements correlated well, Tables 7, 8 and 9. Details of the fracture toughness testing are included in Appendix 2.

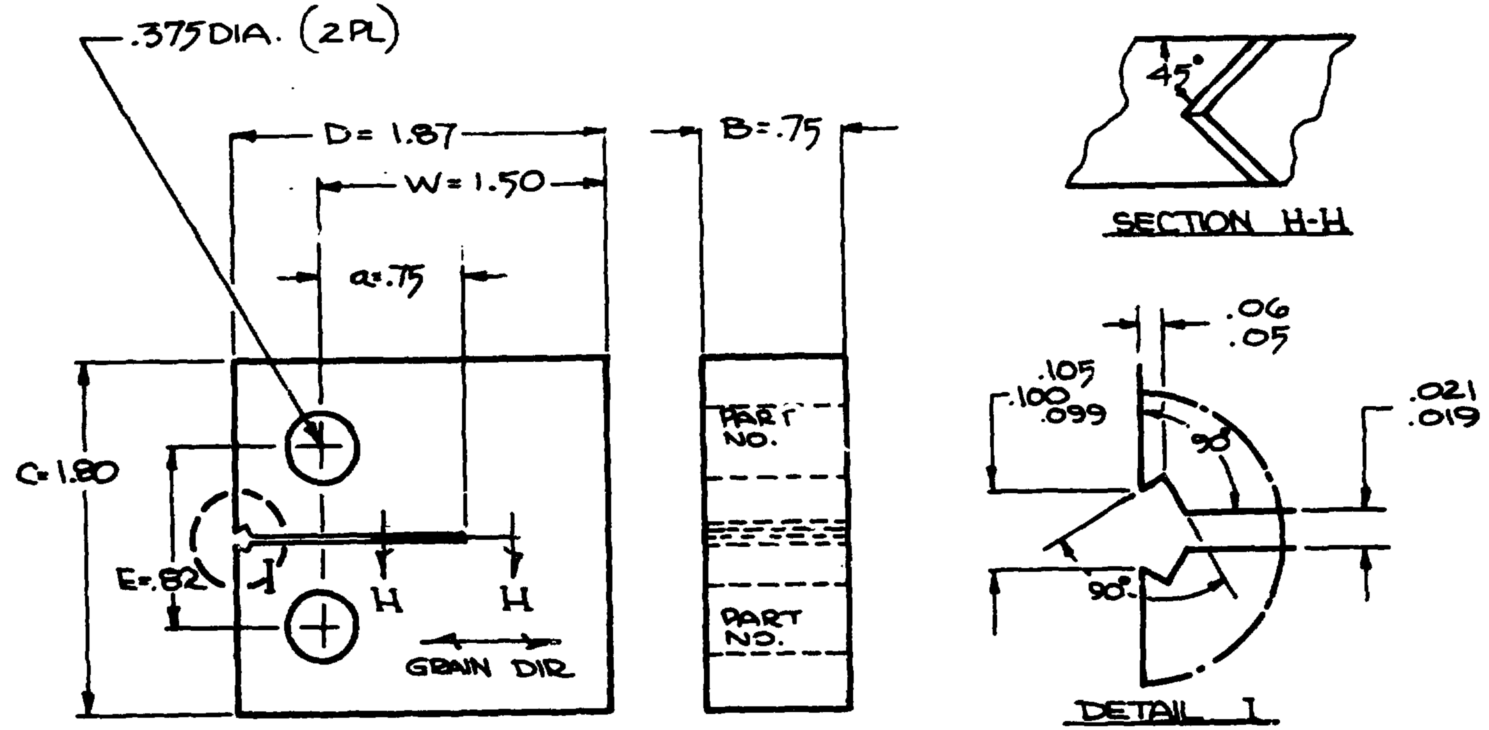

Figure 7. Compact Tension Specimen

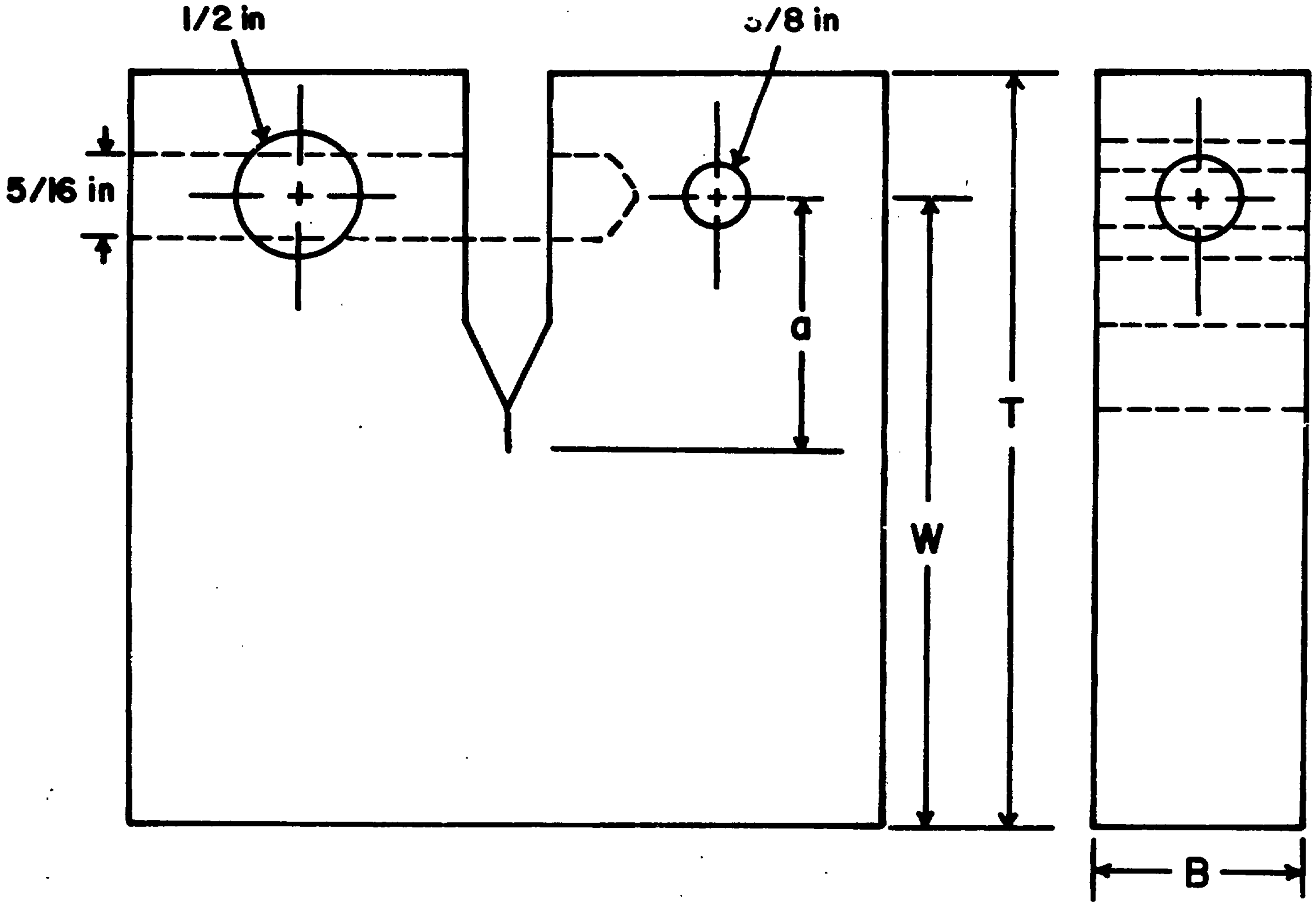

FIGURE 8. BOLT-LOADED COMPACT TENSION SPECIMEN USED AT UNIVERSITY OF FLORIDA.

Figure 9. Bolt-loaded fracture toughness specimens exposed in chloride solution were used in tests at University of Florida to assess the influence of the inhibitors on the crack growth rate, K_{Iscc} and hydrogen content of test alloys.

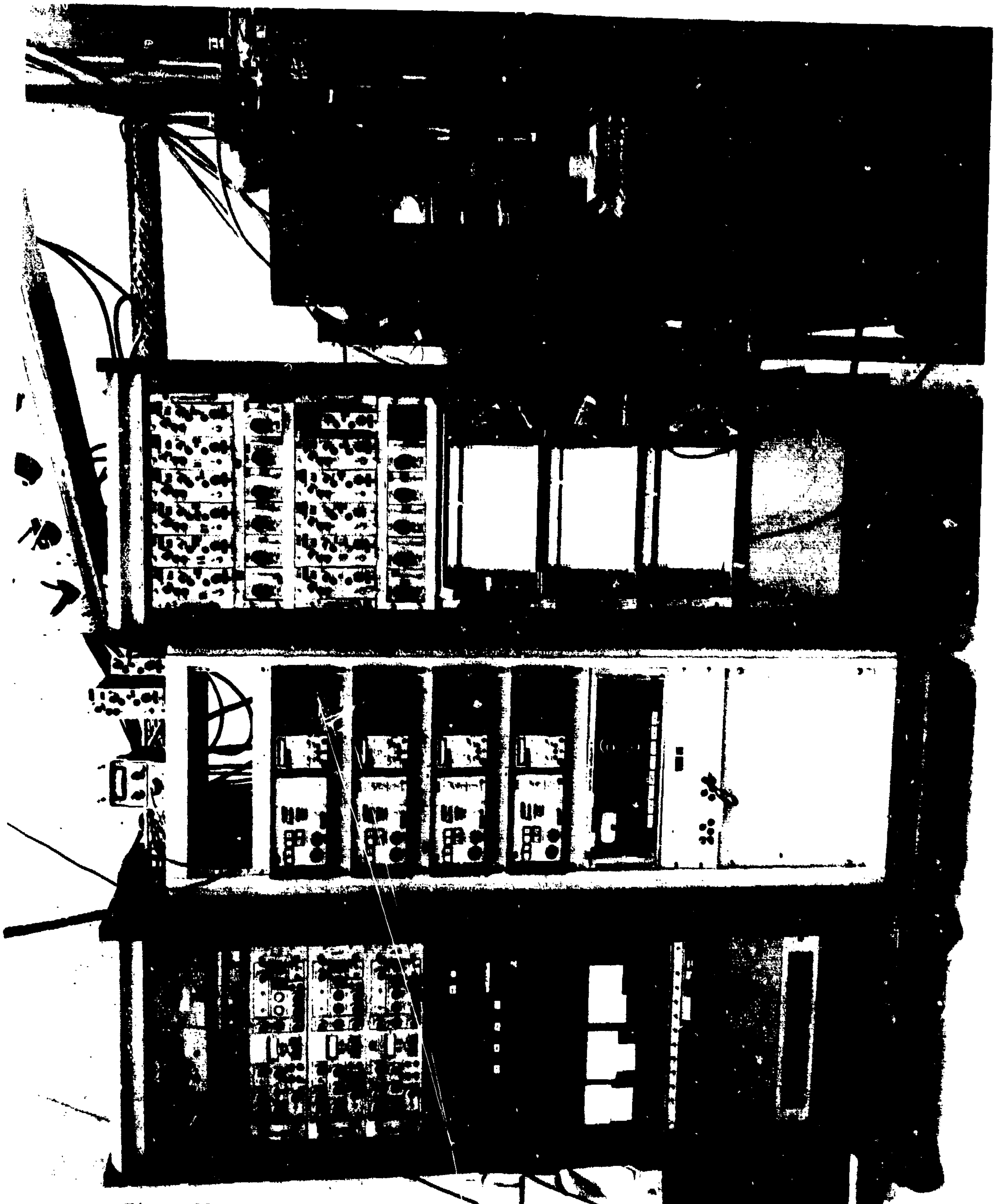

Figure 10. Equipment array employed at Boeing Aerospace Corporation to conduct fracture toughness studies.

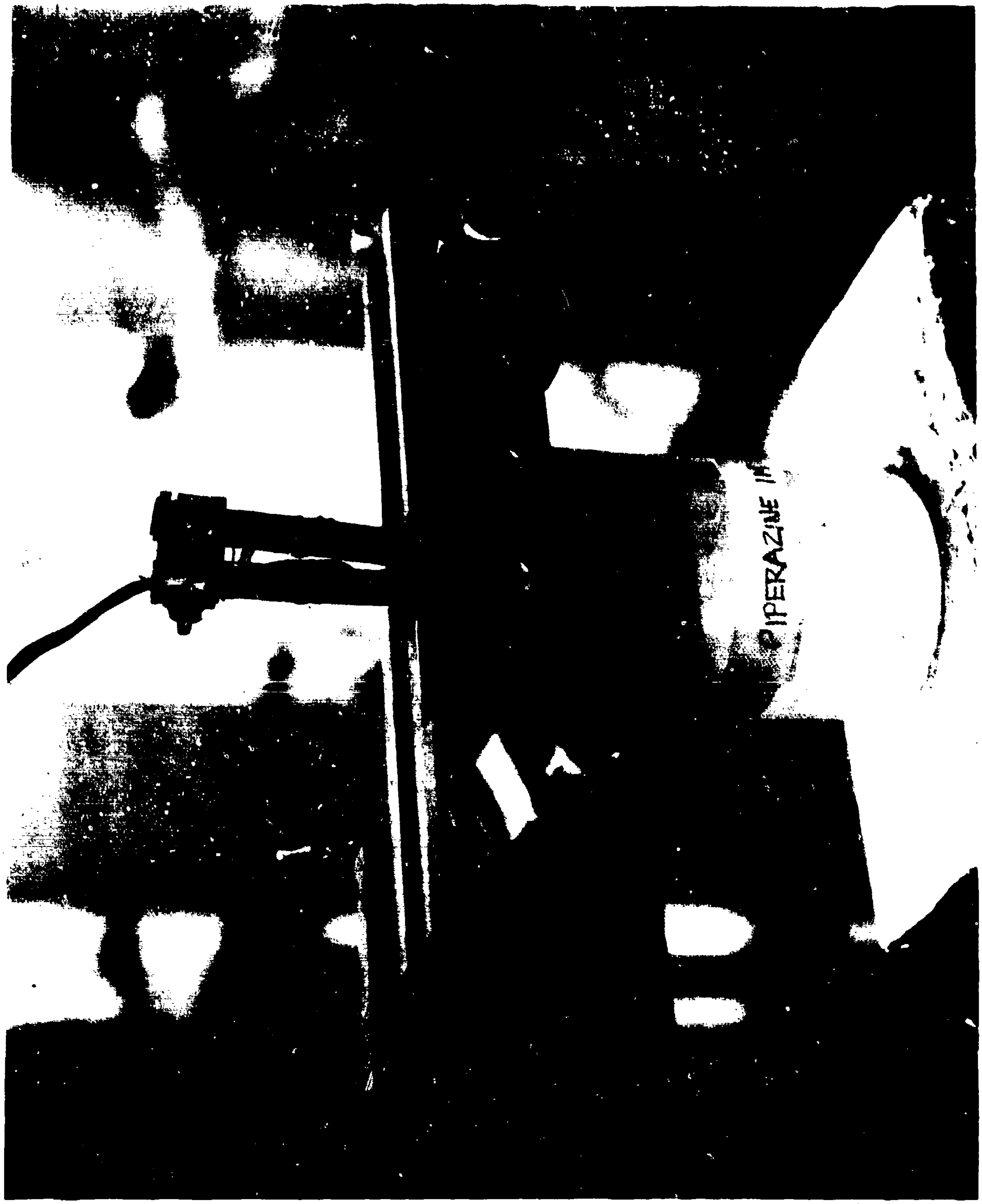

Figure 11. Close-up of testing of fracture toughness specimen in inhibited chloride solution at Boeing Aerospace Corporation.

3.3.2. Hydrogen Analysis - It was the original plan to make hydrogen analyses of exposed test specimens both at University of Florida and at Boeing Company, so that a comparision could be made between the LECO Hydrogen Analyzer and Dr. K. B. Das' Ultrasensitive Hydrogen Analysis Apparatus. Unfortunately, the LECO apparatus was unadaptable to the configuration of specimens at University of Florida and full reliance had to be made on Dr. Das' apparatus to determine hydrogen content, both of samples from the Boeing tests and from samples exposed at University of Florida. It is not surprising that samples which had to be shipped from Gainesville to Seattle for analysis gave some evidence of loss of hydrogen en route despite the fact that considerable effort was made to minimize such loss through use of dry-ice packing and insulated containers. The details of operations of the ultrasensitive hydrogen detector are given in Appendix 2.

TABLE 7

FRACTURE TOUGHNESS BEHAVIOR OF AEROSPACE ALLOYS IN CHLORIDE SOLUTIONS CONTAINING NALCO 39L AS AN INHIBITOR

0.1 $\bar{M}$ Cl^- IN DISTILLED WATER WITH (X) STOCK SOLUTION NALCO 39L ADDED

Specimen 4340 #		Inhibitor Conc.† (X) Stock Solution	K_{Ii} (ksi$\sqrt{in}$)	K_{failed} (ksi$\sqrt{in}$)	K_{Iscc} (ksi$\sqrt{in}$)	da/dt (in/min)	Hydrogen Level ppm	E_{corr}/E_{H_2} (SCE)	Remarks
C4-10	(F)*	None	~20	---	<10	---	1.49 FPC 2.66 SCG 2.43 BM	---	
C4-25	(B)*	None	~10	~10	~10	$3x10^{-3}$	2.15 FPC 5.15 SCG 2.06 BM	---	
C4-26	(B)	0.01	~10	11	<11	$1.7x10^{-4}$	0.71 FPC 1.30 SCG 0.85 BM	---	
C4- 8	(F)	0.1	~20	---	~15	---	1.79 FPC 1.38 SCG 1.42 BM	---	
C4-13	(F)	0.1*	~15	---	~10	---	1.60 FPC 1.91 SCG 0.94 BM	-0/78/-0.72	Cathodically protected (Potentiostat)
C4-12	(F)	0.5	~12	---	~12	---	1.42 FPC 1.65 SCG 1.73 BM	---	

*(F) = University of Florida
(B) = Boeing Aerospace Corporation

† Nalco 39L is a proprietary combination of several ingredients; therefore, concentration is expressed in terms of percent of "Stock Solution" (considered to be 1.0 x SS).

TABLE 7 (Continued)

Specimen 4340 #		Inhibitor Conc.† (X) Stock Solution	K_{Ii} (ksi$\sqrt{in}$)	K_{failed} (ksi$\sqrt{in}$)	K_{Iscc} (ksi$\sqrt{in}$)	da/dt (in/min)	Hydrogen Level ppm	E_{corr}/E_{H_2} (SCE)	Remarks
C4-19	(F)	1.0	~15	---	~10	---	1.52 FPC 3.47 SCG 1.61 BM	---	
C4-33	(B)	1.0	~10	~15	~14	$1.5x10^{-4}$	1.41 FPC 1.43 SCG 0.89 BM	---	No Cl^- in solution
C4-20	(F)	1.0	~12	---	<10	---	2.22 FPC 2.02 SCG 1.30 BM	-0.48/-0.84	Magnesium anode
C4-21	(F)	1.0	~12	---	~12	---	0.37 FPC 0.39 SCG 1.01 BM	-0.47/-0.84	Zinc anode
<u>9-4-30</u>									
CH- 6	(B)	None	---	---	<44	$5x10^{-4}$	5.16 FPC 3.75 SCG 1.59 BM	---	
CH- 7	(B)	1.0	40	58	~57	$1x10^{-6}$	0.81 FPC 2.33 SCG 1.34 BM	---	

TABLE 7 (Concluded)

Specimen 300M #		Inhibitor Conc.† (X) Stock Solution	K_{Ii} (ksi$\sqrt{in}$)	K_{failed} (ksi$\sqrt{in}$)	K_{Iscc} (ksi$\sqrt{in}$)	da/dt (in/min)	Hydrogen Level ppm	E_{corr}/E_{H_2} (SCE)	Remarks
C3-12	(B)	None	~12	~18	~16	$1x10^{-3}$	1.60 FPC 2.01 SCG 1.64 BM	---	
C3-13	(B)	0.01	16	~16	~15	$1.2x10^{-3}$	1.49 FPC 0.67 SCG 1.08 BM	---	
C3-15	(B)	0.10	17	~17	~15	$2.0x10^{-3}$	0.56 FPC 0.63 SCG 1.46 BM	---	
C[illegible]	(F)	0.10	~20	---	~14	---	3.02 FPC 2.55 SCG 2.11 BM	---	
<u>17-4 PH</u>									
C1- 4	(F)	None	71	71	>71	---	---	---	
C1-12	(B)	None	59	67	~58	$1.2x10^{-3}$	1.77 FPC 1.64 SCG 1.19 BM	---	
C1-13	(B)	0.1	66	74	73	$8.3x10^{-7}$	1.23 FPC 0.90 SCG 1.07 BM	---	No rust
C1- 3	(F)	0.1	71	71	>71	---	---	---	

TABLE 8

FRACTURE TOUGHNESS BEHAVIOR OF AEROSPACE ALLOYS IN CHLORIDE SOLUTIONS CONTAINING PIPERAZINE AS AN INHIBITOR

0.1 $\bar{M}$ Cl^- IN DISTILLED WATER WITH (X) $\bar{M}$ PIPERAZINE ADDED

Specimen 4340 #		Inhibitor Conc.	K_{Ii} (ksi$\sqrt{in}$)	K_{failed} (ksi$\sqrt{in}$)	K_{Iscc} (ksi$\sqrt{in}$)	da/dt (in/min)	Hydrogen Level ppm	E_{corr}/E_{H_2} (SCE)	Remarks
C4-25	(B)*	None	∿10	∿10	∿10	$3x10^{-3}$	2.15 FPC 5.15 SCG 2.06 BM	---	
C4-10	(F)*	None	∿20	---	<10	---	1.46 FPC 2.66 SCG 2.43 BM	---	
C4- 3	(F)	0.01 $\bar{M}$	∿40	---	∿10	---	--- 2.24 SCG 1.29 BM	---	
C4-27	(B)	0.01 $\bar{M}$	∿10	∿10	∿10	$1.8x10^{-3}$	.082 FPC 1.31 SCG 1.11 BM	---	
C4-34	(B)	1.0 $\bar{M}$	∿10	71	61	$<1x10^{-6}$	1.99 FPC 3.22 SCG 1.94 BM	---	No rust
<u>300M #</u>									
C3-11	(B)	1.0 $\bar{M}$	15	∿56	∿55	$8.3x10^{-7}$	1.01 FPC 3.41 SCG 0.97 BM	---	No rust
C3-12	(B)	None	12	∿18	∿16	$1x10^{-3}$	1.60 FPC 2.01 SCG 1.64 BM	---	

*(F) = University of Florida
(B) = Boeing Aerospace Corporation

TABLE 8 (Concluded)

Specimen 9-4-30		Inhibitor Conc.	K_{Ii} (ksi$\sqrt{in}$)	K_{failed} (ksi$\sqrt{in}$)	K_{Iscc} (ksi$\sqrt{in}$)	da/dt (in/min)	Hydrogen Level ppm	E_{corr}/E_{H_2} (SCE)	Remarks
CH- 6	(B)	None	---	---	<44	$5x10^{-4}$	5.16 FPC 3.75 SCG 1.59 BM	---	
CH- 8	(B)	1.0	40	57	~57	$1x10^{-6}$	1.24 FPC 1.14 SCG 1.14 BM	---	No rust
17-4 PH									
C1- 4	(F)	None	~71	~71	<71	---	---	---	
C1-12	(B)	None	59	67	~58	$1.2x10^{-3}$	1.97 FPC 1.65 SCC 1.19 BM	---	
C1-14	(B)	1.0	66	79	78	$8.3x10^{-7}$	2.22 FPC 2.02 SCG 3.05 BM	---	No rust

TABLE 9

FRACTURE TOUGHNESS BEHAVIOR OF AEROSPACE ALLOYS IN CHLORIDE SOLUTIONS CONTAINING PIPERIDINE AS AN INHIBITOR

0.1 $\bar{M}$ Cl^- IN DISTILLED WATER WITH (X) $\bar{M}$ PIPERIDINE ADDED

Specimen 4340 #	Inhibitor Conc.	K_{Ii} $(ksi\sqrt{in})$	K_{failed} $(ksi\sqrt{in})$	K_{Iscc} $(ksi\sqrt{in})$	da/dt (in/min)	Hydrogen Level ppm	E_{corr}/E_{H_2} (SCE)	Remarks
C4-10 (F)*	None	~20	---	<10	---	1.49 FPC 2.66 SCG 2.43 BM	---	
C4-25 (B)*	None	~10	~10	~10	$3x10^{-3}$	2.15 FPC 5.15 SCG 2.06 BM	---	
C4-28 (B)	0.01 $\bar{M}$	~10	~10	~10	$2.5x10^{-3}$	1.01 FPC 3.03 SCG 1.17 BM	---	
C4- 6 (F)	0.1 $\bar{M}$	~20	---	<10	---	2.81 FPC 2.47 SCG 1.75 BM	---	
C4-14 (B)	1.0 $\bar{M}$	~10	~21	~21	$8x10^{-5}$	1.15 FPC 4.19 SCG 1.98 BM	---	
<u>9-4-30</u>								
CH- 6	None	---	---	<44	$5x10^{-4}$	5.16 FPC 3.75 SCG 1.59 BM	---	
CH- 9	1.0	42	56	~55	$1x10^{-6}$	1.37 FPC 1.20 SCG 1.95 BM	---	No rust

*(F) = University of Florida
(B) = Boeing Aerospace Corporation

TABLE 9 (Concluded)

Specimen 300M #		Inhibitor Conc.	K_{Ii} (ksi$\sqrt{in}$)	K_{failed} (ksi$\sqrt{in}$)	K_{Iscc} (ksi$\sqrt{in}$)	da/dt (in/min)	Hydrogen Level ppm	E_{corr}/E_{H_2} (SCE)	Remarks
C3-12	(B)	None	∿12	∿18	∿16	$1x10^{-3}$	1.60 FPC 2.01 SCG 1.64 BM	---	
C3- 6	(F)	None	∿23	---	∿22	---	1.49 FPC 4.02 SCG 1.76 BM	---	
C3- 4	(F)	0.01 $\bar{M}$	∿23	---	∿22	---	1.55 FPC 2.95 SCG 1.45 BM	---	Crack branching observed
C3-10	(B)	1.0 $\bar{M}$	∿15	∿61	∿60	$8.3x10^{-7}$	2.30 FPC 0.93 SCG 1.33 BM	---	No rust
17-4 PH									
C1- 4	(F)	None	∿71	∿71	>71	---	---	---	
C1-12	(B)	None	59	67	∿58	$1.2x10^{-3}$	1.77 FPC 1.64 SCG 1.19 BM	---	
C1- 2	(F)	0.1	∿71	∿71	>71	---	---	---	

SECTION 4

RESULTS

Tables 7, 8 and 9 summarize the fracture toughness, crack growth rate and hydrogen analysis data from Phase III of this investigation. The distribution of test work gave greatest emphasis to alloy 4340 in an attempt to provide a "bridge" between alloys known to suffer hydrogen embrittlement damage and other alloys thought to be less susceptible.

SECTION 4.1

ALLOYS 4340 AND 300M (300M IS GROUPED WITH 4340 BECAUSE IT IS COMPOSITIONALLY EXCEEDINGLY CLOSE TO 4340 AND ITS BEHAVIOR PROVED TO BE ESSENTIALLY THE SAME.)

The effect of the inhibitors on the fracture toughness behavior in 0.1 M chloride solutions is as follows. The polyfunctional inhibitor, Nalco 39L, reduces the hydrogen content of the metal as compared to samples where no inhibitor was present in the chloride solution. The hydrogen level at (or near) the fracture surface was consistently lower for samples exposed to 39L than for piperidine or piperazine. Nalco 39L (at the concentration recommended by the manufacturer) also decreases the crack growth rate by about 1 order of magnitude. Increasing the inhibitor concentration <u>increases</u> hydrogen content monotonically without materially changing K_{Iscc}. Comparing the nil-chloride data with 0.1 M chloride data it is observed that chloride ion also increases the hydrogen content and decreases K_{Iscc}. The crack growth rate for 4340 is slightly higher than that for 300M in Nalco 39L. This inhibitor is most effective in the concentration recommended by the manufacturer. If the concentration is <u>too dilute</u>, or <u>too concentrated</u>, the effectiveness <u>decreases</u> significantly. The reduction in hydrogen content upon use of the inhibitor corresponds with the fact that the electrode potential of 4340 (and 300M) exposed to Nalco 39L is above the equilibrium hydrogen line. Piperazine also reduces hydrogen entry at all concentration levels tested in 0.1 M chloride solutions (but not to quite as low levels as Nalco 39L). The range of inhibitor concentrations was from .01 M to 1.0 M. The .01 M piperazine addition was insufficient to retard crack growth rate or to increase K_{Iscc} significantly as compared to samples in which no inhibitor was added, thus the reduction of hydrogen apparently was insufficient to affect these other criteria, Figure 11. By contrast, at 1.0 M concentration of piperazine, the crack growth rate was reduced by 3 orders of magnitude to less than 1×10^{-6} inch per minute and K_{Iscc} was increased from 10 for the uninhibited solution to 61 for the inhibited solution.

Piperidine appears to take somewhat longer to provide effective inhibition of 4340 in solutions in the range of .01 M to 1.0 M in 0.1 M chloride solutions. However, after its effect has been established, results are essentially the same as for piperazine. That is to say, the .01 M piperidine reduces hydrogen entry but does not reduce crack growth rate or increase K_{Iscc} but the 1.0 M solution significantly reduces crack growth rate and increase K_{Iscc}. The detailed evidence in Table 9 indicates that the effects are slightly less than for piperazine, Table 8. The results with 300M are similar. It is particularly interesting to observe that for both piperazine and piperidine (both "blocking" inhibitors) the hydrogen levels as determined at (or near) the fracture surface of fracture toughness samples exposed to 1.0 M additions of the inhibitor in chloride solution were <u>significantly higher</u> than for the corresponding tests using Nalco 39L. Nonetheless, piperazine and piperidine were both significantly more effective in inhibiting cracking of 4340 and 300M (alloys known to be especially subject to hydrogen embrittlement) than was Nalco 39L. This leads to the speculation that there may be hydrogen either combined or trapped in the surface film which is prevented from entering the metal as a result of use of piperazine or piperidine. Further research will be necessary to elucidate the mechanism involved here. Cathodic protection tests with 4340 in 39L indicate that the crack growth rate can be arrested in 39L by the use of zinc anodes. Thus, evidence is available that cracking of 4340 in solutions containing chlorides and (highly concentrated) Nalco 39L may crack by active path corrosion rather than by hydrogen embrittlement. Apparently the inhibitor prevents the hydrogen charging of 4340 even when cathodic protection is applied so long as the level of cathodic protection is modest. This implies that zinc or possibly aluminum anodes could be useful whereas magnesium anodes should not be used. This is consistent with work reported by Das et. al.[15] who reported that use of cathodic protection could be beneficial for such alloys. The fact that the mode of failure of 4340 and 300M may be changed from hydrogen embrittlement to active path corrosion by choice of the concentration of the inhibitor offers an unusual opportunity to study the mechanisms involved.

Fractographs were made of compact fracture toughness specimens of 4340 alloy exposed to Nalco 39L of two concentrations of piperazine, .01 M and 1.0 M. Electron microscope replica pictures of the fracture surfaces of specimens C4-27 and C4-34 appear as Figures 12 and 13. Both fractographs are from the slow crack growth (SCG) region. At the lower concentration of inhibitor, the details of the fractograph reveal intergranular cleavage typical of hydrogen embrittlement failure. By contrast, at the higher concentration the features

Figure 12. Replica of slow crack growth (SCG) region of specimen C4-27, alloy 4340 exposed to 0.1 M chloride solution containing 0.01 M piperazine. This level of inhibitor did not increase K_{Iscc} and features of the fracture surface show intergranular cleavage.

C4-27

11,200 X

Figure 13. Replica of slow crack growth (SCG) region of specimen C4-34, 4340 alloy exposed to 0.1 M chloride solution containing 1.0 M piperazine. Although hydrogen content in the SCG region was above base-line, K_{Iscc} increased to 61 ksi $\sqrt{inch}$ and features of the fracture surface show considerable dimpled character as compared with Figure 12.

C4-34

11,200 X

indicate quasi-cleavage and have considerable dimpled character indicating a change in mode. The fractographs offer additional evidence that the mode of failure is affected by the chemical environment for 4340.

Confirmation that a protective barrier film forms in the presence of piperazine or piperidine is given by Figure 14. These samples were exposed in 1.0 M piperazine and piperidine for a period of approximately a month and then were allowed to stand in laboratory ambient air for another month before the pictures were taken. Comparing these samples, it is clear that piperazine provides a protective barrier coating (when present in sufficient concentration) which retards corrosion.

SECTION 4.2

ALLOY HP 9-4-30

HP 9-4-30 is a structural alloy of considerably lower strength than 4340 or 300M. The data contained in Table 7 shows that Nalco 39L is quite attractive as an inhibitor for HP 9-4-30. As with other alloys, piperidine and piperazine are not useful at low concentrations such as .01 M, however, at 1.0 M concentrations, the crack growth rate is in the range of 10^{-6} inches per minute and K_{Iscc} increases to 55 or above with very low hydrogen in the samples. It would appear that any of the 3 inhibitors would be suitable for this alloy provided the concentration level was adequate.

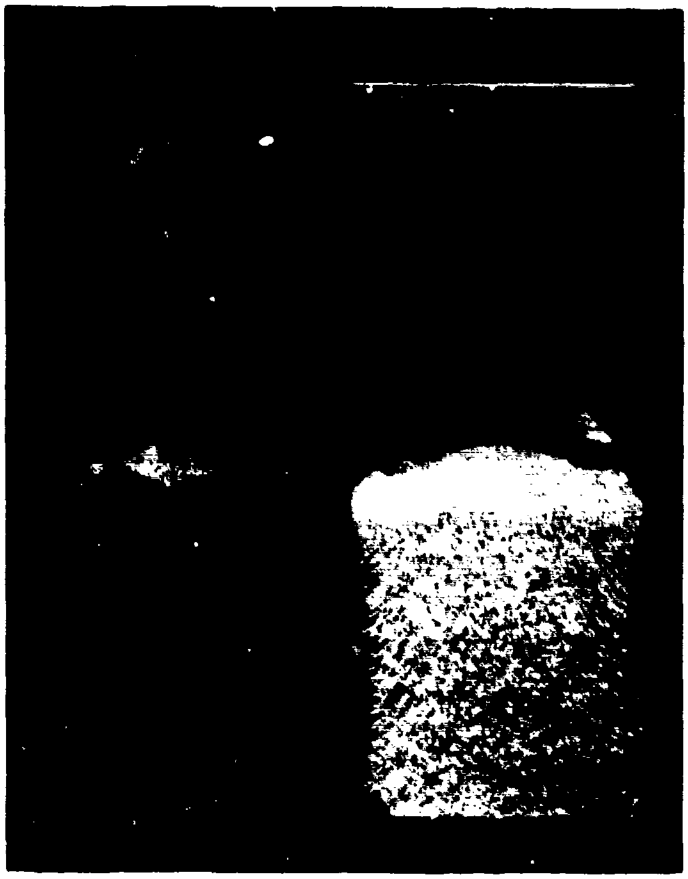

C4-27 C4-34

~ 2X

Figure 14. Comparison of the fracture surfaces of C4-27 and C4-34 after approximately one month exposure to laboratory atmosphere reveal that 1.0 M piperazine (specimen C4-34) leaves a protective barrier coating of considerable persistance as shown by its freedom from rusting.

SECTION 4.3

ALLOY 17-4 PH

This alloy is exceedingly sensitive to the presence of hydrogen and the data in Table 7 agree with data of Das et. al.[14] Even the dilute concentration of Nalco 39L reduced hydrogen levels in 17-4 PH by approximately 50% and raised the K_{Iscc} value approximately to K_{Ic}. Inasmuch as 17-4 PH is particularly sensitive to hydrogen, an inhibitor which should be most successful with this alloy would be one which minimizes the possibility of hydrogen entry. Nalco 39L would appear to be somewhat preferable to the blocking inhibitors (piperidine and piperazine) for this alloy since use of Nalco 39L consistently resulted in lowest hydrogen content. It is possible that the blocking inhibitors could be manipulated by the addition of recombination catalysts to encourage the formation of molecular hydrogen at the surface, thereby preventing the danger of entry. This, of course, would require considerable research.

SECTION 4.4

ALLOY HY180

This alloy was added late in the program on the basis that work would be done on it insofar as time and resources permitted. As a consequence, no data are presented for this alloy.

SECTION 5

DISCUSSION OF RESULTS AND CONCLUSIONS

Starting with nearly 200 inhibitor formulations, a selection process has been employed which narrowed the number of alternatives under consideration to three. These were piperazine, piperidine and Nalco 39L. Each of these inhibitors has successfully survived the go and no-go tests referred to herein as the dip test, and also show the proper change in polarization resistance suggesting that instantaneous corrosion rates are significantly reduced using these formulations. Piperazine and piperidine appear to function as blocking inhibitors and when available in sufficient concentration reduce the hydrogen level, reduce the crack growth rate and increase the K_{Iscc} values for fracture toughness specimens of each of the alloys tested. The numerical value of the measured hydrogen content from fracture surfaces is higher for either piperidine or piperazine than for Nalco 39L. It is postulated that this is the result of a surface-effect possibly involving either chemical or mechanical attachment of hydrogen to the passivating barrier film. The polyfunctional inhibitor Nalco 39L reduces hydrogen levels to the lowest value of the 3 inhibitors used in fracture toughness tests. Apparently, Nalco 39L does not deposit a significantly protective barrier film (as compared to the blocking inhibitors). Nalco 39L is most effective at the concentration recommended by the manufacturer. At lower concentrations it is not particularly effective and at higher concentrations crack growth rates actually increase apparently by a change in mechanism. Fractographic evidence and response to cathodic protection suggests that at higher concentrations the cracking is active path cracking rather than hydrogen embrittlement, for alloy 4340 exposed to Nalco 39L. The ability to manipulate the mode of fracture by altering the concentration of this inhibitor offers a unique opportunity to study the mechanism of hydrogen embrittlement and active path corrosion.

SECTION 6

NEW DIRECTIONS FOR RESEARCH

In the conduct of the current research it became evident that the process of selecting inhibitor candidates could be improved if additional, scientifically-based screening processes were developed. Concurrently with the present investigation a number of preliminary studies were made in an attempt to develop alternate screening methods. Those which appeared to show particular promise and deserve further development include the study of the influence of inhibitors on the NMR shift, the effect of wetability of the surface as measured by changes in the contact angle (as influenced by inhibitor additions), and the study of the importance of the zeta potential using streaming potential apparatus. Another type of experiment which should be considered is the study of the mechanism of inhibition by making use of cathodic protection as a tool to investigate the capacity of adsorbed films to prevent hydrogen entry. As a corollary to such studies it may be possible to incorporate a hydrogen recombination catalyst in the structure of the adsorbed film. The ability to control the mode of cracking of 4340 by varying the concentration of Nalco 39L offers a unique opportunity to elucidate the mechanisms of hydrogen embrittlement and active path corrosion.

Maitra[16] has made use of "growth path envelope" techniques to analyze the behavior of materials under conditions leading to pitting. Such an analysis on materials exposed to inhibited versus uninhibited electrolytes could lead to an assessment of whether the inhibitor functions primarily to reduce the likelihood of <u>initiation</u> of pitting or whether its function is primarily one of <u>changing the magnitude</u> of the intensity of the corrosion process.

REFERENCES

1. P. A. Parrish, "The Retardation of Crack Propagation for High Strength Low Alloy Steels in Aqueous Media by Addition of Oxidizing Inhibitors," Ph.D. Dissertation, University of Florida, June 1974.
2. P. A. Parrish, C. M. Chen and E. D. Verink, Jr., "Retardation of Crack Propagation for D6AC High Strength, Low-Alloy Steel in Aqueous Media by Addition of Oxidizing Inhibitors," Stress Corrosion-New Approaches ASTM STP 610 Amer. Soc. for Testing and Materials, 1976, pp. 189-198.
3. J. M. Johnson, "Use of the Experimental Potential-pH Diagram for D6AC Steel to Interpret Its Corrosion Behavior in Aqueous Media," M.S. Thesis, University of Florida, June 1974, included in Report No. AFML-TR-76-8, February 1976.
4. M. Pourbaix, 1970 Corrosion Research Conference of NACE, Philadelphia, March 2-4, 1970, and in a number of later literature citations.
5. B. F. Brown, C. T. Fuju and E. F. Dahlberg, JECS, 116, 2, Feb. 1969, p. 218.
6. J. A. Smith, M. H. Peterson and B. F. Brown, Corrosion, 26, 12, Dec. 1970.
7. A. R. Troiano, TASM, 52, 54, 1960.
8. B. F. Brown, "Stress Corrosion Cracking and Related Phenomena in High Strength Steels," Naval Research Laboratory Report 6041, Nov. 6, 1963.
9. K. B. Das, "An Ultrasensitive Hydrogen Detector," ASTM STP 543, 1974, pp. 106-123.
10. J. I. Bregman, Corrosion Inhibitors, MacMillan Company, New York, 1963.
11. C. T. Lynch, K. J. Bhasoali and P. A. Parrish, "Inhibition of Crack Propagation of High Strength Steel Through Single and Multifunctional Inhibitors," Report No. AFML-TR-76-120, August 1976.

12. E. D. Verink, Jr. and M. Pourbaix, "Use of Electrochemical Hysteresis Techniques in Developing Alloys for Saline Exposures," Corrosion, 27, 12, December 1971.

13. K. D. Efird and E. D. Verink, Jr., "The Crevice Protection Potential for 90-10 Copper Nickel," Corrosion, 33, 9, September 1977.

14. N. I. Sax, Dangerous Properties of Industrial Materials, 2nd Ed., Reinhold Publishing Corporation, New York, 1963.

15. K. B. Das, W. G. Smith, R. W. Finger and J. N. Masters, "Hydrogen Embrittlement of Cathodically Protected 15-5 pH Stainless Steel," Presented at the Second International Congress on Hydrogen in Metals, Paris, France, June 6-11, 1977.

16. S. Maitra, "Initiation and Propagation of Pits on Aluminum," Ph.D. Dissertation, University of Florida, June 1974.

17. L. Raymond, Effects of Chemical Environment on Fracture Processes, Proceedings of Third Tewksbury Symposium on Fracture, pp. 159-169, C. S. Osborne and R. C. Gifkins, Editors, The Faculty of Engineering, Melbourne, Australia, June 4-6, 1974.

APPENDIX A

Heat treatment of fracture toughness specimens was in accordance with, and extracted from, the following Boeing Aircraft Company specifications:

Material	Heat Treatment Specifications
4340	BAC 5617
300M	"
HP 9-4-30	"
17-4 PH	BAC 5619

Excerpted from BAC Specification 5617

6.2 **PROCESS CONTROL REQUIREMENTS**

6.2.1 **TEMPERATURE REQUIREMENTS FOR HEAT TREATING PROCESSES**

Select the correct temperature for the required process from Table V.

TABLE V
TEMPERATURE REQUIREMENTS FOR VARIOUS HEAT TREATING PROCESSES FOR DESIGNATED STEELS

Temperature °F [1]				Minimum Tempering Temperature °F for Tensile Strength Range Shown [2]					
Steel Type	Subcritical Anneal	Normalize	Harden	125-145 KSI Rc 27-33	150-170 KSI Rc 34-38	160-180 KSI Rc 36-40	180-220 KSI Rc 40-43	200-220 KSI Rc 43-46	220-240 KSI Rc 46-48
4130, 8630	1250-1300	1600-1700	1550-1600	1050	900	800	725		
4135, 8735	1250-1300	1600-1700	1550-1600	1100	925	825	750		
4137, 4037	1225-1275	1600-1700	1550-1600	1100	950	825	750		
4140, 8740	1225-1275	1600-1675	1525-1575	1100	1000	925	850	725	
4340	1225-1275	1600-1650	1500-1550	1100	1025	925	875	725	
4330M (BMS 7-122)	1225-1275	1650-1700	1550-1600		1050	950	850	675	500
AMS 6407	1225-1275	1650-1700	1550-1600		1050	925	825	650	500
4335M	1225-1275	1625-1675	1550-1625		1125	1025	950		
6150 [3]	1225-1275	1600-1650	1550-1600		950		800	700	
1065, 1070 [3]	1225-1275	1550-1650	1450-1525		950		775	675	
1095 [4]	1225-1275	1500-1600	1450-1525		950		800	700	
4340 AMS6414 BMS 7-51, MIL-S-5000 MIL-S-8844	1225-1275	1600-1650	1500-1550	Double temper at 400 minimum for 260-280 KSI					
4340M	1250-1300	1625-1700	1575-1625	Double temper at 575 for either 270-300 KSI or 275-300 KSI. The tempering facility shall be set at a temperature of 575.					
5Cr-1.3Mo	1375-1425	[5]	1825-1875	See 6.2.6.3 for Tempering.					
52100	1225-1275	1600-1700	1500-1550	Temper at 350 minimum for Rockwell C 60-65					
Mn-Si-Ni MIL-S-7108 AMS6418	1175-1225 [6]	1675-1725	1575-1625	[7]					
9Ni-4Co-.20C (BMS 7-182, Type IV)	1100-1300 [9]	1625-1675	1525-1575	Double temper at 1025-1075 for 190 KSI minimum [8]					
9Ni-4Co (BMS 7-182, Type II)	1100-1300 [9]	1675-1725	1500-1550	Double temper at 1000 for 220 KSI minimum. The tempering facility shall be set at a temperature of 1000. [8]					
D6AC	1225-1275	1700-1750	1675-1725	See 6.2.7 for 195-220 KSI, Rockwell C 42-46.					

BAC 5617
PAGE 7

REV. (B) 10-8-64 (E) 11-3-70 (K) 10-26-76

ORIGINAL ISSUE

6.2.1 (Continued)

[1] The maximum difference in temperature between the control instrument setting and all points within the working zone of the furnace is ± 25 F. The control instrument shall therefore be set at a temperature which will ensure that all points in the working zone are within the temperature range specified.

[2] The temperatures shown except for 9Ni-4Co (BMS 7-182, Type II) and 4340M are the minimum temperature control instrument settings allowed for the specific steel and strength range shown. It will usually be necessary to compensate for size effects and variation in composition of individual heats of steel. In general, a tempering temperature approximately 50 F higher than the minimum shown will be necessary to achieve the required tensile strength.

[3] For Spring temper Rc 43-47, temper at 725F to 900F.

[4] For Spring temper Rc 40-46, temper at 700F to 800F.

[5] Normalizing process not applicable to 5Cr-1.3Mo material.

[6] Hold for 15-20 hours. For best machinability heat at 1360-1380F for a time sufficient to insure through heating, cool at 50F per hour to 1100F, air cool to room temperature, reheat to 1175 to 1225F for 15 to 20 hours and air cool.

[7] 225-235 KSI minimum 600F
230-240 KSI minimum 500F
235-245 KSI minimum 400F

[8] Hold at -100F or colder prior to any tempering operations. The soak time begins after the cooling facility has recovered to the specified temperature. If the parts are immersed in liquid cooling medium (i.e., acetone, alcohol, trichloroethylene), soak 15 minutes minimum for section thicknesses up to 0.50 inches and add 15 minutes for each additional 0.01 - 0.50 increment of thickness. If parts are cooled in a gaseous medium (i.e., air, nitrogen) soak 30 minutes minimum for thicknesses up to 0.50 inches and add 30 minutes for each additional 0.01 - 0.50 inch increment of thickness. Gaseous cooling medium is preferred over liquid cooling medium because the former reduces the danger of cracking due to a slower rate of cooling.

[9] A double subcritical anneal treatment is required to obtain a hardness not greater than BHN 341 or equivalent. Conduct the first subcritical anneal at 1250-1300F and the second subcritical anneal at 1100-1150F.

6.2.2 TIME REQUIREMENTS FOR HEAT TREATING PROCESSES

Select the appropriate time for the required process from Table VI.

TABLE VI

MINIMUM TIME REQUIREMENTS FOR VARIOUS HEAT TREATING PROCESSES BASED ON SECTION THICKNESS, TYPE OF FURNACE, TYPE OF STEEL AND STRENGTH LEVEL

Section Thickness In Inches [1]	Minimum Heating Time In Minutes For Normalizing or Hardening [2]				Minimum Heating Time In Hours for Tempering Or Subcritical Annealing [2]					
	Atmosphere Furnace		Salt Bath		Circulating Air Furnace			Salt Bath		
	[3] [6]	5Cr-1.3Mo [6]	[3]	5Cr-1.3Mo	Up to 220 KSI [4] [5]	220-240 KSI	Over 240 KSI [7]	Up to 220 KSI	220-240 KSI	Over 240 KSI [7]
Up to 0.100	20	20	17	17	1-1/2	2-1/2	3	1-1/4	2-1/2	2-1/2
0.101-0.250	25	20	18	18	1-1/2	2-1/2	3	1-1/4	2-1/2	2-1/2
0.251-0.500	45	20	35	20	1-1/2	2-1/2	3	1-1/4	2-1/2	2-1/2
0.501-1.00	60	30	40	20	2	3	4	1-1/2	2-3/4	3
1.01 -1.50	75	30	45	20	2-1/4	3-1/4	4-1/2	1-1/2	2-3/4	3-1/4
1.51 -2.00	90	45	50	25	2-1/2	3-1/2	5	1-3/4	3	3-1/2
2.01 -2.50	105	45	55	25	2-3/4	3-3/4	5-1/2	1-3/4	3	3-3/4
2.51 -3.00	120	60	60	30	3	4	6	2	3-1/4	4
	Time For 3 Inches Plus Indicated Time for Each Additional Half Inch									
Over -3.00	15	7-1/2	5	5	1/4	1/4	1/2	1/8	1/8	1/4

REV (B) 10-8-64 (D) 3-1-67 (E) 11-3-70 (K) 10-26-76

ORIGINAL ISSUE 1-6-60

6.2.2 (Continued)

1 A complex part may be considered as being comprised of a series of blocks; each block having a given length, width, and thickness (smallest dimension). Define section thickness as the largest thickness in this series of blocks - for single layer loading. For multilayer loading the thickness shall be defined as the smallest of the three dimensions and the maximum of this dimension used for section thickness. If straightening fixtures are used during tempering, consider the section thickness of the fixture in addition to that of the part.

2 For air furnaces, heating time (soak period) begins when the coldest work zone recorder thermocouple reading reaches the minimum of the heat-treating range after insertion of the load. For salt baths or lead baths, time begins when the control temperature returns to the minimum of the heat-treating range being used.

3 This column applicable to all materials and heat-treat ranges except hardening of 5Cr-1.3Mo. This column is also applicable to preheating or subcritical annealing of 5Cr-1.3Mo steel at 1450F or intermediate heat-treat at 1650F.

4 This column also applicable to preheating of 5Cr-1.3Mo at 1200F.

5 This column applicable to subcritical annealing.

6 For copper plated parts increase minimum heating time by 50 percent.

7 The following curve may be used for determination of tempering times on 4340M steel parts.

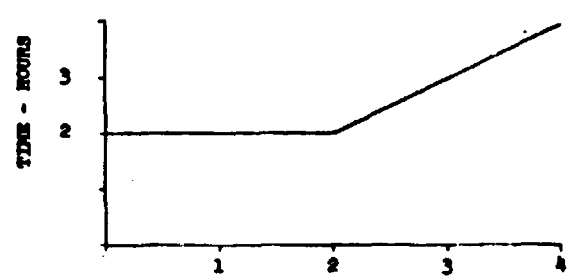

6.2.3 SUBCRITICAL ANNEALING

6.2.3.1 General

a. Temperature and time requirements for subcritical annealing are as shown in Tables V and VI. At the conclusion of the heating period remove the parts from the furnace and cool in still air.

b. As combustible atmospheres containing hydrogen cannot safely be used at temperatures below 1300F, subcritical annealing should ordinarily be conducted in air and the scale removed by pickling or mechanical cleaning. Where the scale produced cannot be tolerated, special methods such as using an inert atmosphere or a plating of copper 0.0005 inches minimum thickness according to BAC 5756, Type III may be applicable. Consult the Materials Technology Organization for specific applications.

Excerpted from BAC Specification 5617

6.2.3.2 <u>Subcritical Annealing Application</u>

a. Subcritical annealing may be used for the following:

(1) Annealing between forming operations.

(2) Stress relief prior to hardening for the removal of machining or forming stresses.

(3) Removal of prior heat treatment where necessary in rework of excessively warped parts.

b. Subcritical Annealing is required prior to further processing of normalized high hardenability steels such as 4340, 4330M, AMS 6407, 4335M, HMS 7-26 and 9Ni-4Co. Following normalizing, air cool the parts to approximately 160F maximum, and then subcritical anneal within one hour.

Note: If hardening is to follow immediately after normalizing, subcritical anneal may be omitted by preheating parts at the subcritical annealing temperature for a time sufficient to insure through-heating, then transfer to the hardening furnace.

BAC
5617
PAGE 10

Excerpted from BAC Specification 5619

REV (A) 11-4-63 (B) 6-19-64 (B)

6.4.2 PROCESS REQUIREMENTS FOR THE HEAT TREATMENT OF 17-7PH

6.4.2.1 <u>Annealing to Condition A</u>

a. Reannealing is required only for the following.

(1) Parts fusion welded in the annealed condition.

(2) Rework of previously heat-treated parts.

(3) Parts for which the time limit for transformation has been exceeded.

BAC
5619
PAGE 9

ORIGINAL ISSUE 1-6-60

6.4.2.1 (Continued)

b. Reanneal as needed for:

(1) The removal of cold work between forming operations.

(2) The control of distortion during heat treatment.

c. Where required, anneal as follows:

(1) Charge cold part into a furnace at 1925 - 1975F.

(2) Hold for 3 minutes minimum to 7 minutes maximum per 0.1 inch section thickness or fraction thereof, but not less than 3 minutes.

(3) Remove from the furnace and cool in still air. Cool to below 1200F within 30 minutes after removal from the furnace.

6.4.2.2 <u>Removal of Annealing Scale</u>

After final annealing and prior to austenite conditioning descale parts annealed during fabrication in accordance with BAC 5751.

6.4.2.3 <u>Austenite Conditioning</u>

a. Austenite condition by heating the material at 1375-1425F for 90 minutes.

b. Air cool to 212F maximum prior to transformation treatment.

6.4.2.4 <u>Transformation to Condition T</u>

a. Transformation shall be accomplished by cooling the parts below 60F within one hour after removal from the 1400F furnace. The parts shall be maintained below this temperature for not less than 30 minutes.

b. Parts may be straightened during cooling from the 1400F austenite conditioning treatment. Transformation to a martensitic structure accompanied by growth of the material and decreased ductility begins at approximately 200F. Where due to straightening operations, the one hour time limit for attaining 60F cannot be met, cool the parts within 72 hours, to minus 20F ± 10F for 3 hours prior to precipitation hardening.

6.4.2.5 <u>Removal of Condition T Scale</u>

After transformation treatment to Condition T and before precipitation hardening to Conditions TH1060 or TH1110, remove scale resulting from austenite conditioning at 1400F in accordance with BAC 5751.

Option: If protective coating is used on the part, scale resulting from the 1400F austenite conditioning may be removed after TH Hardening Treatment.

When heat-treat scale can be completely removed following hardening, scale resulting from the 1400F Austenite conditioning treatment may be removed after hardening.

6.4.2.6 <u>Hot Straightening During Precipitation Hardening</u>

Straightening may be accomplished by the use of special fixtures during Precipitation Hardening to Condition TH1060 or TH1110.

6.4.2.7 <u>Precipitation Hardening to Condition TH1060 or TH1110</u>

a. Precipitation harden to Condition TH1060 (180-200 KSI, R_c40-43) by heating parts to 1050-1080F for 90 minutes and air cool.

b. Precipitation harden to Condition TH1110 (150-170 KSI, R_c34-38) by heating the parts to 1100-1120F for 90 minutes and air cool.

c. Reheat-treat parts having hardness in excess of the specified maximum for an additional 90 minutes at a higher temperature to obtain the required hardness. An increase in temperature of 10F will result in a decrease in hardness of one R_c point. Do not reheat above 1140F.

REV (A) 11-4-63 (B) 6-19-64 (C) 11-24-64 (E) 7-13-70

6.4.2.7 (Continued)

d. Parts having hardness less than the specified minimum may be reworked as follows:

(1) Parts having a hardness of up to one R_c division less than the specified minimum may be reheated 890-910F for 30 minutes to recover the required strength.

(2) Where the treatment described above is inadequate, reannealing at 1950F is required prior to reprocessing. The precipitation hardening temperature may be reduced from that previously used, but in no instance shall the initial temperature be less than 1040F.

6.4.2.8 Removal of Condition TH Scale

Remove all traces of heat treatment scale in accordance with BAC 5751.

6.4.2.9 Precipitation Hardening to Condition RH950

Heat treatment to Condition RH950 shall be accomplished in accordance with the requirements of 6.4.3.3 - 6.4.3.7 inclusive except heat treated properties shall be as follows:

Thickness (In.)	Tensile Strength (KSI)	Hardness (R_c)
0.0015 - 0.1874	210 - 230	44 - 47
0.1875 - 0.6250	200 - 220	43 - 46

6.4.2.10 Precipitation Hardening to Condition CH900 (R_c 46 Minimum)

Precipitation harden to Condition CH900 by heating the parts to 890 - 910F for 60 minutes and air cool. (Starting material must be purchased in Condition C).

6.4.2.11 Removal of Condition CH900 Scale

Remove all traces of heat treatment scale in accordance with BAC 5751.

APPENDIX B

ULTRASENSITIVE HYDROGEN DETECTION SYSTEM

Hydrogen Analysis System

A general view of the Ultrasensitive Hydrogen Detector appears as Figure 15. A schematic of the hydrogen detector is shown in Figure 16. The system essentially consists of an airtight specimen holder which is placed inside the work coil of an induction heater for the purpose of extracting hydrogen from the test specimen, a micro-quantitative gas metering system or MGM system, a semi-permeable membrane (from here on referred to as SPM), a vac-ion pump, and a source of high purity argon gas. Hydrogen present as water, organic material as well as elemental, is released from a metal by heating the metal. The hydrogen thus liberated is directed toward the activated SPM by the flowing argon gas (carrier gas). The SPM lets only hydrogen permeate through it while remaining impermeable to other gases. On the other side of the SPM is a continuously pumped high vacuum chamber (ion-pump housing). Thus, the SPM has a high vacuum on one side and about one atmosphere pressure on the other.

The pressure in the ion-pump chamber is measured by monitoring the ion-current through the pump. Once the chamber is pumped down to its base vacuum, any permeation of hydrogen through the SPM will result in an increase in the ion-current reading as seen by the ion-pump. An increase in the ion-current reading is therefore directly proportional to the amount of hydrogen in the carrier gas stream. Thus, if the detector readout is calibrated by introducing known amounts of hydrogen in the vacuum system, thereby establishing a relation-

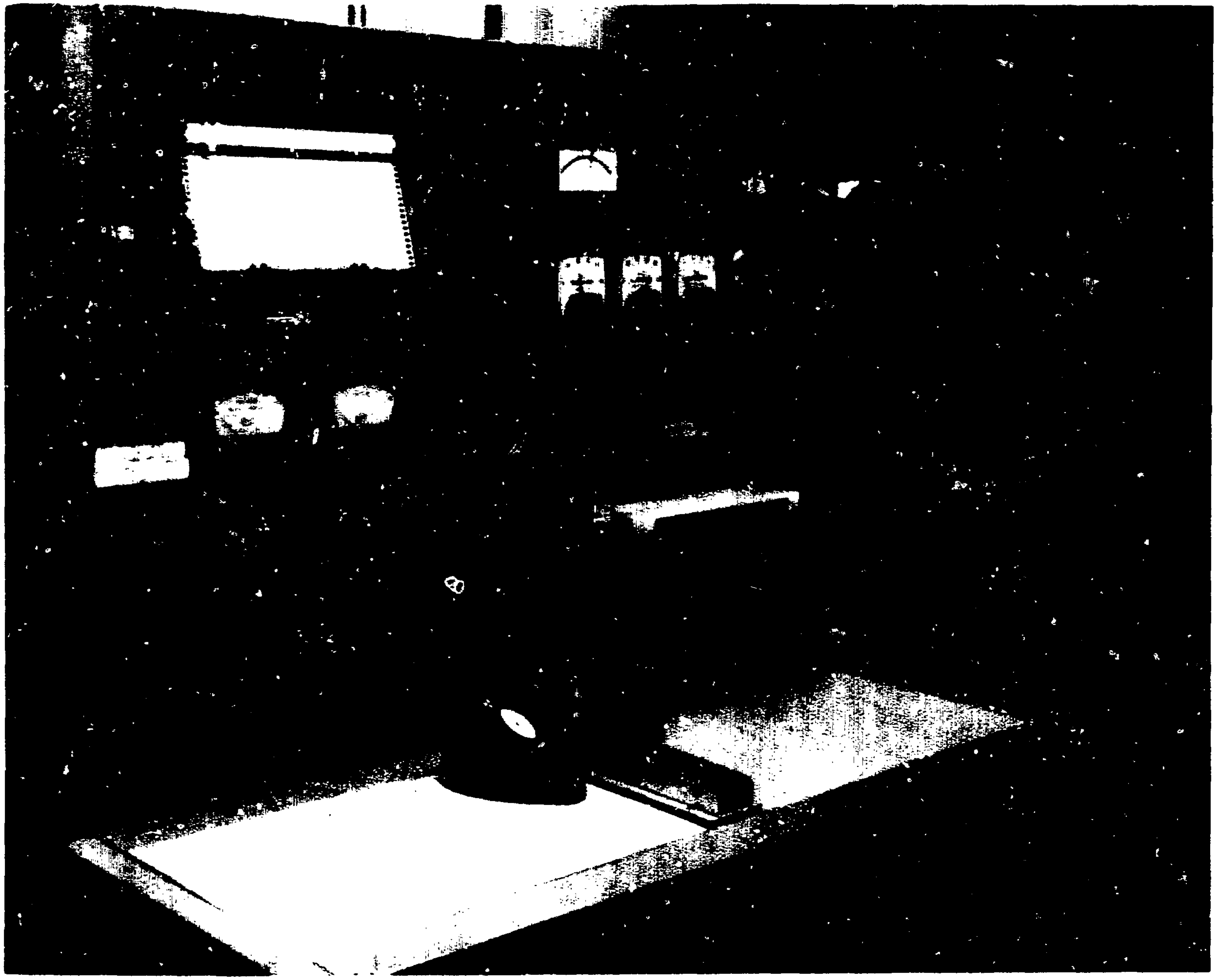

Figure 15. General view of Ultrasensitive Hydrogen Detector of Boeing.

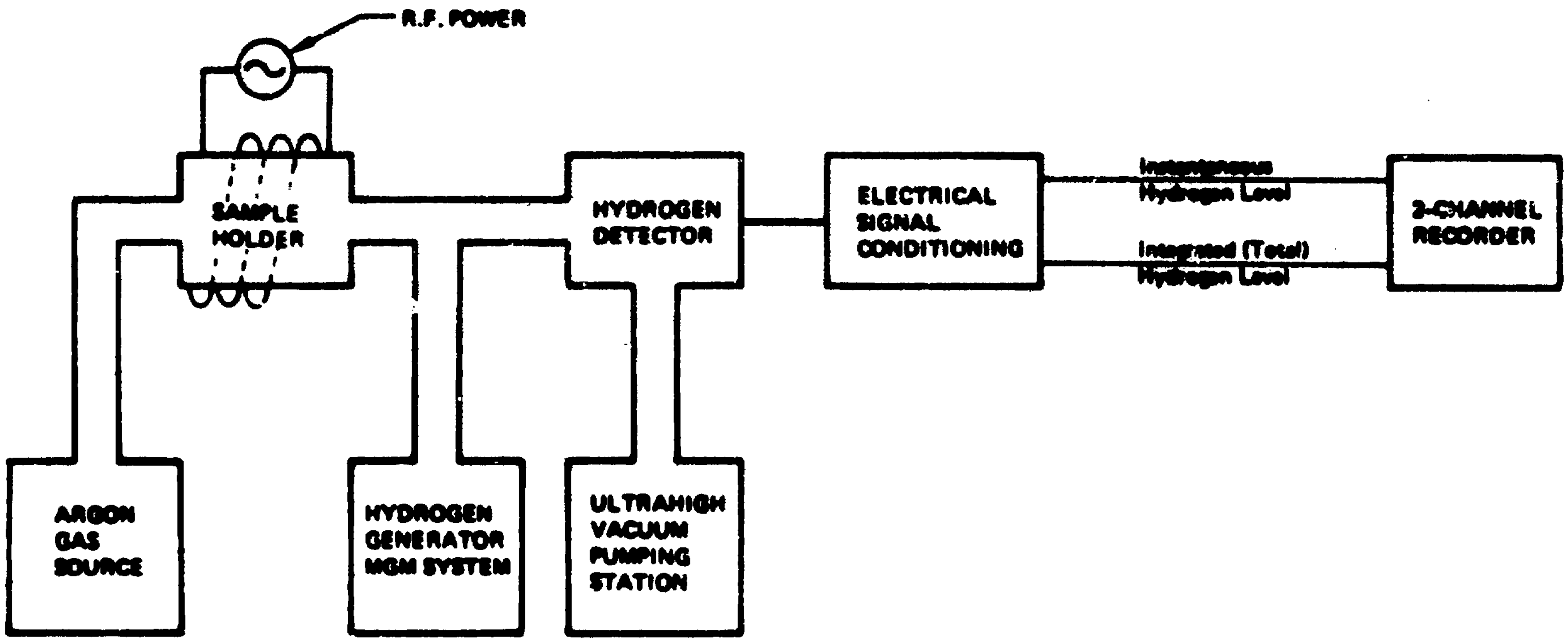

Figura 16. Schematic of hydrogen detector.

ship between the concentration of hydrogen in the gas stream and the ion-current readings, one can easily estimate the amount of hydrogen in the gas stream from an unknown source. In the present case the detector is calibrated by introducing known amounts of hydrogen in the vacuum chamber by the MGM system, and a relationship is established between the concentration of hydrogen in the gas stream and the ion-current readings. Such a calibration procedure also provides a check for the linearity of the detector and gives a measure of its sensitivity. The sensitivity of the detector depends upon the flow-rate of the carrier gas, and the temperature of the SPM. Thus, in order to maintain the same permeation efficiency for hydrogen from the MGM system and the test specimen it is essential to keep these parameters constant.

For bulk hydrogen analysis the experimental approach essentially consists of extracting hydrogen from the test specimens using an induction furnace and then measuring the amount of hydrogen thus extracted with the hydrogen detector. Hydrogen, after permeating through the SPM, arrives in the detector housing where it is detected by an appropriate sensing element and an instantaneous electrical signal representative of the amount of hydrogen present is recorded. In practice when the specimen is heated, the time for complete extraction of hydrogen depends upon the rate at which hydrogen diffuses out of the specimen. This rate of diffusion is proportional to the temperature of the specimen and as such the time required for complete extraction of hydrogen depends on how rapidly the temperature of the specimen is raised. In the case of bulk hydrogen analysis the instantaneous hydrogen signal generally traces out a Maxwellian type of curve representing complete extraction of hydrogen from the test specimen. When this curve is integrated electronically it results in an S-shaped curve giving a direct numerical value for the area under the Maxwellian curve.

The design of the system is such that not all the hydrogen directed toward the SPM goes through the detector. Moreover, the diffusion of hydrogen through SPM itself is a time dependent process. When using an induction furnace, such factors are eliminated by following a special operating technique. Here the sample is heated to its melting point in a programmed manner and held at this temperature until complete extraction of hydrogen is accomplished. Both the instantaneous and integrated hydrogen signals are recorded as a function of time. Following the hydrogen extraction, at the same carrier gas flow-rate $(dv/dt)_{Ar}$, a known amount of hydrogen is introduced into the gas stream from the MGM system for a precisely known time Δt. The MGM system consists of a pinched capillary tubing with one of its ends connected to the carrier gas channel and the other connected to a high purity hydrogen bottle, a low pressure gas regulator, and gas bleed-off system. By regulating the hydrogen gas pressure, varying amounts of hydrogen can be introduced into the carrier gas stream. The rate of hydrogen gas flow through the pinched capillary is determined by connecting it to a glass capillary tubing (of precisely known dimensions) containing a little slug of mercury. From the knowledge of the area of cross-section of the glass capillary and the time taken for the mercury column to move a given distance, the rate $(dV/dt)_H$ is computed. The ratio of $(dV/dt)_H$ and $(dV/dt)_{Ar}$ then gives a measure of ppm of hydrogen in the carrier gas stream. It should be noted that $(dV/dt)_H \approx 10cc^{-4}/_{min}$ is much smaller than $(dV/dt)_{Ar} \approx 100cc/_{min}$. Furthermore, the product of $(dV/dt)_H$, Δt, and density of hydrogen "ρ"$_H$ gives the amount of hydrogen M, in grams, introduced into the gas stream in time Δt. The units of the integrated signal are coulombs. Thus, if the integrated signal from the known hydrogen input M_1 (grams) and the test sample are Q_1 and Q_2 coulombs respectively, the amount of hydrogen M_2 (grams) from the test sample can be calculated from the relation $M_2 = (Q_2/Q_1)M_1$.

To further illustrate the method of analysis an example of a (certified) NBS sample is given here which has a known hydrogen concentration of 32 ± 2 ppm. After pumping the detector housing down to its base level a carrier gas flow-rate of 50 cc/min was chosen for the experiment. Thereafter, hydrogen was extracted from the NBS sample by heating the specimen in the induction furnace. The time for complete extraction from this sample, which weighed 0.1847 gms, was about 16 minutes. The integrated hydrogen signal gave a value of 190400 microcoulombs. Thereafter, by appropriately regulating the hydrogen gas pressure on the MGM system and maintaining the same carrier gas flow-rate of 50 cc/min, hydrogen was introduced into the argon gas stream at the rate of 19.05×10^{-3} cc/min for 4.0 minutes. In other words, in 4 minutes, 6.38×10^{-6} grams of hydrogen was introduced into the gas stream. This gave an integrated hydrogen signal of 207000 microcoulombs. Using the relation

$$\frac{207000 \times 10^{-6} \text{ coul}}{5.38 \times 10^{-6}} = \frac{190400 \times 10^{-6} \text{ coul}}{X \text{ grams}}$$

$$\text{or } X = 5.869 \times 10^{-6} \text{ grams,}$$

the total bulk hydrogen in the NBS sample was found to be 5.869×10^{-6} grams. Dividing X by the weight of the sample gives the level of hydrogen in ppm by weight which in this case was 31.78. This value, as can be seen, is well within the uncertainty limits of the NBS sample.

In the present program the test specimens were analyzed for hydrogen content in an identical manner as described above for the NBS specimen. A typical curve for the hydrogen analysis of a NBS standard containing 215 ± 6 ppm hydrogen is shown in Figure 17. During the course of this experimental program certified NBS samples containing 32 ± 2 ppm or 98 ± 5 ppm of hydrogen were analyzed at a schedule of one per week to cross-check the detector's performance and accuracy.

Figure 18 shows schematically the manner of sampling fracture toughness specimens for determination of hydrogen content at (or near) the fracture surface. Hydrogen determinations reported in Tables 7, 8 and 9 were made using this technique.

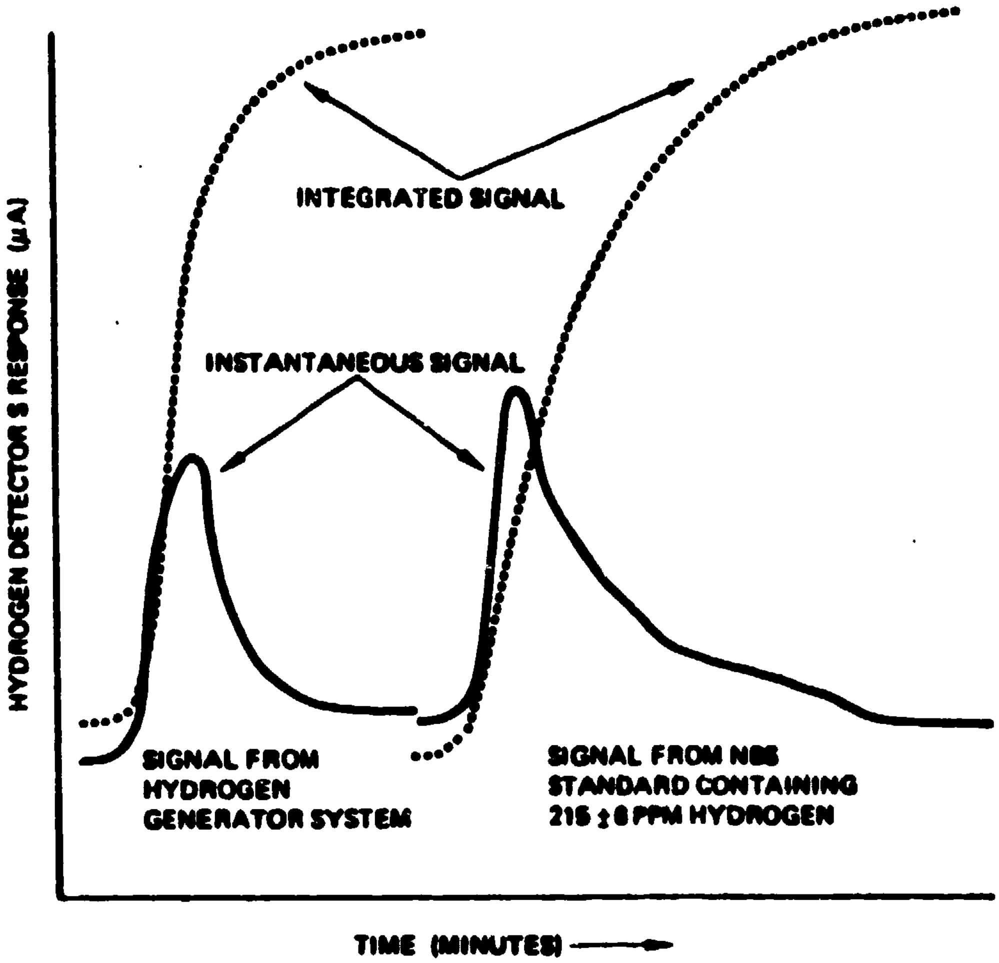

Figure 17. Hydrogen analysis of NBS Standard No. 354 containing 215 ± 6 ppm hydrogen.

SPECIMEN # C4-3

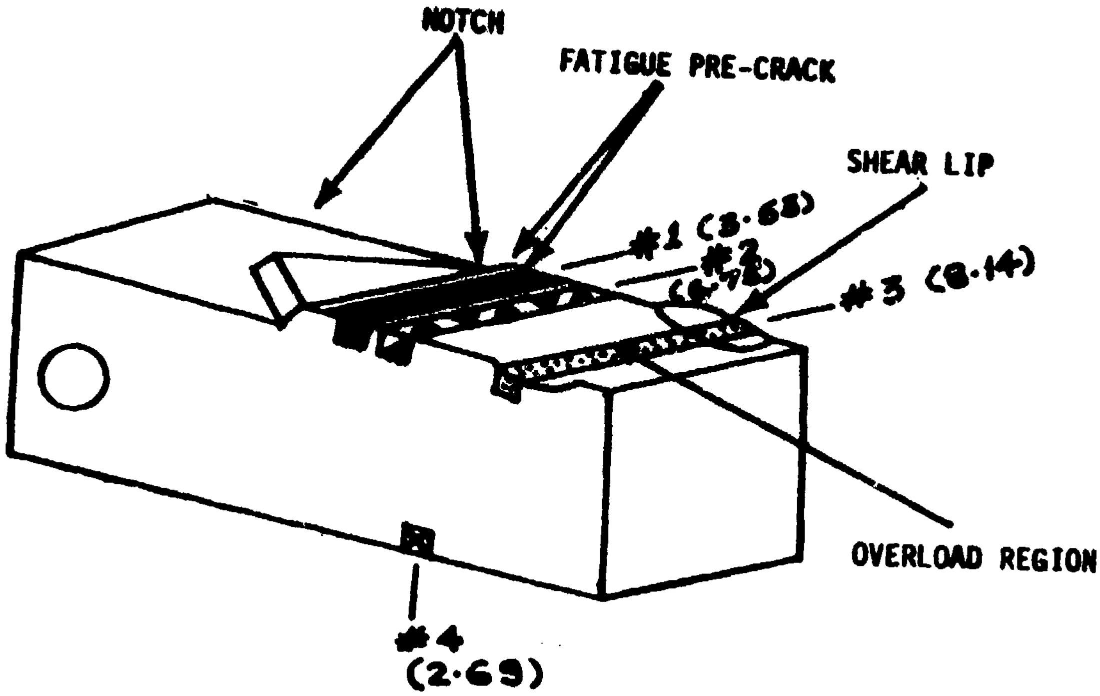

4340 STEEL

Figure 18. Schematic representation of manner of sampling fracture surfaces for hydrogen determination at (or near) the fracture surface using the Ultrasensitive Hydrogen Detector of Das to obtain data for Tables 7, 8 and 9. Figures in parentheses show hydrogen content. This sample was exposed in 0.1 M chloride solution containing 0.01 M piperazine, a concentration of inhibitor too low to be effective. Note hydrogen concentration in slow crack growth (SCG) region and just ahead of the advancing crack are highest.

APPENDIX C

EXPERIMENTAL POTENTIAL VERSUS PH DIAGRAMS FOR TEST ALLOYS

Electrochemical hysteresis methods were used to construct potential versus pH diagrams for each of the alloys tested. The electrolyte in each case was 0.1 M NaCl. The details of the technique are reported elsewhere.[12] Diagrams are shown for 4340, 17-4 PH, HP 9-4-30 and HY180. Because of the similarity between alloys 4340 and 300M, no separate diagram for 300M was constructed.

Figure 19. Experimental potential versus pH diagram fcr alloy 4340 in 0.1 M NaCl solution. Because of the compositional similarity between 4340 and 300M this diagram is considered to apply to 300M as well.

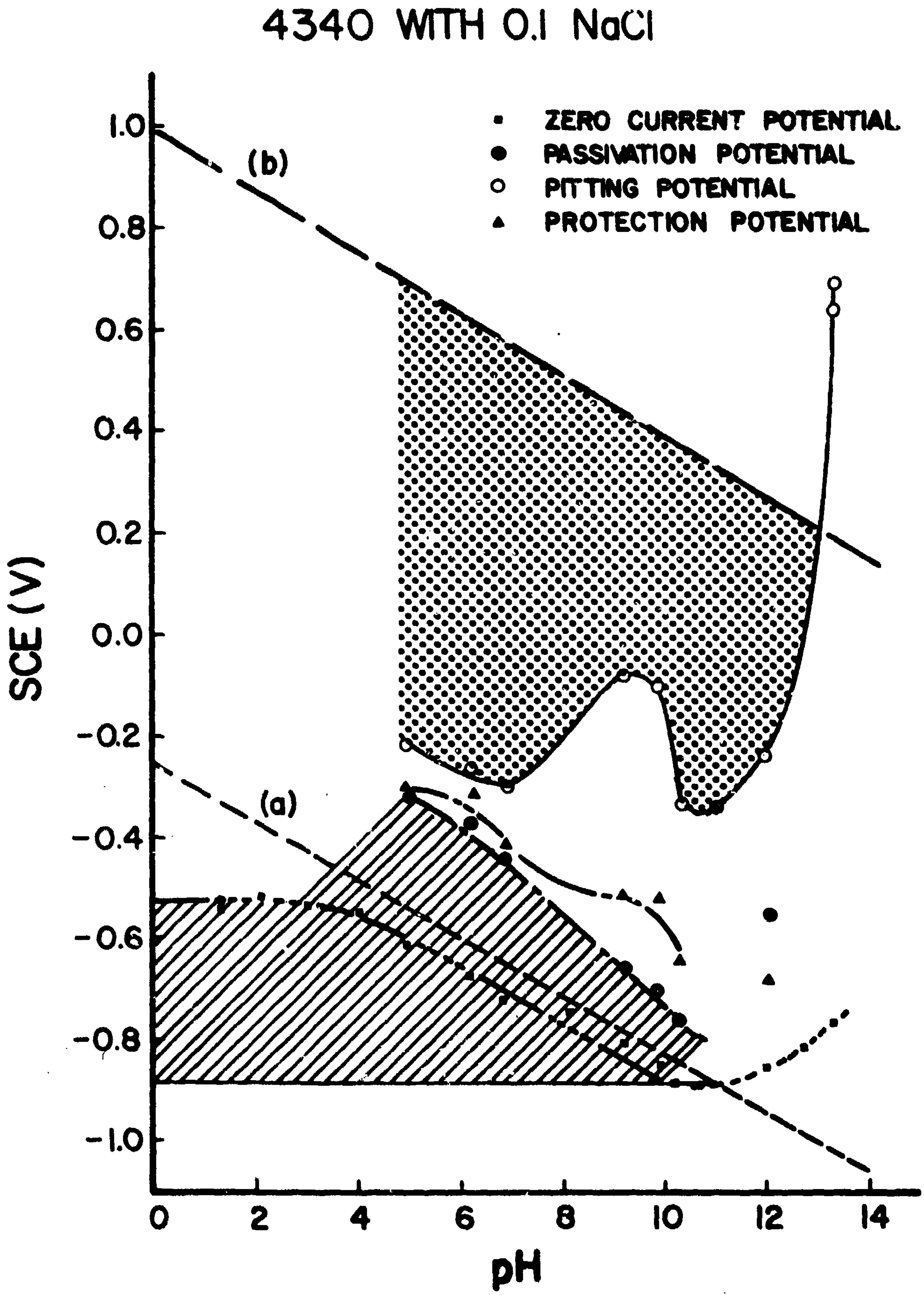

4340 WITH 0.1 NaCl
ZERO CURRENT POTENTIAL
PASSIVATION POTENTIAL
PITTING POTENTIAL
PROTECTION POTENTIAL
(b)
(a)
SCE (V)
1.0
0.8
0.6
0.4
0.2
0.0
-0.2
-0.4
-0.6
-0.8
-1.0
0
2
4
6
8
10
12
14
pH

Figure 20. Experimental potential versus pH diagram for alloy 17-4 PH in 0.1 M NaCl solution. The passive region is considerably more extensive for 17-4 PH than for 4340 or 300M.

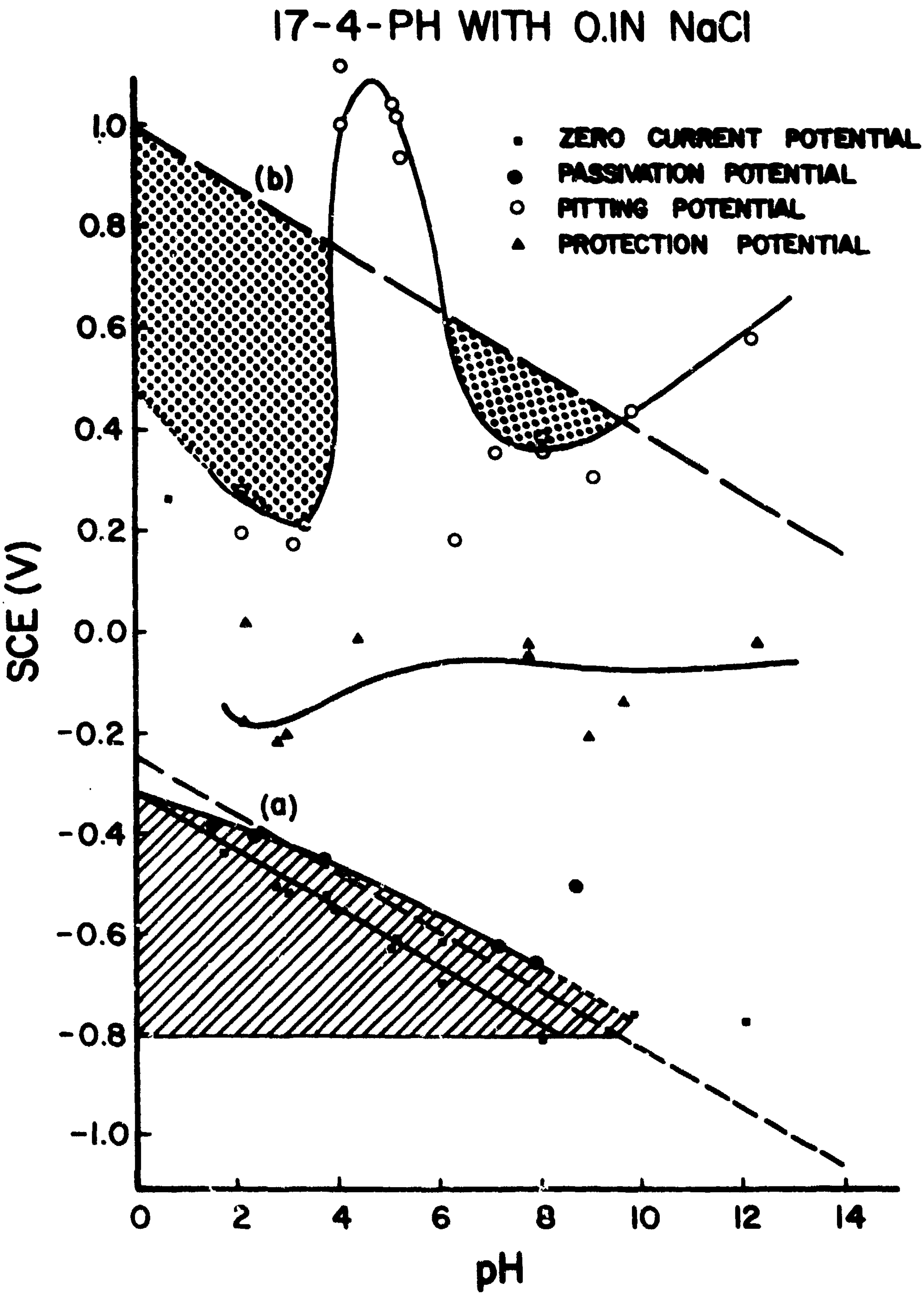

17-4-PH WITH 0.1N NaCl
ZERO CURRENT POTENTIAL
PASSIVATION POTENTIAL
PITTING POTENTIAL
PROTECTION POTENTIAL
(b)
(a)
SCE (V)
1.0
0.8
0.6
0.4
0.2
0.0
-0.2
-0.4
-0.6
-0.8
-1.0
0
2
4
6
8
10
12
14
pH

Figure 21. Experimental potential versus pH diagram for alloy HP 9-4-30 in 0.1 M NaCl solution. This alloy showed considerable tendency to pit, e.g., the passive region was extremely narrow.

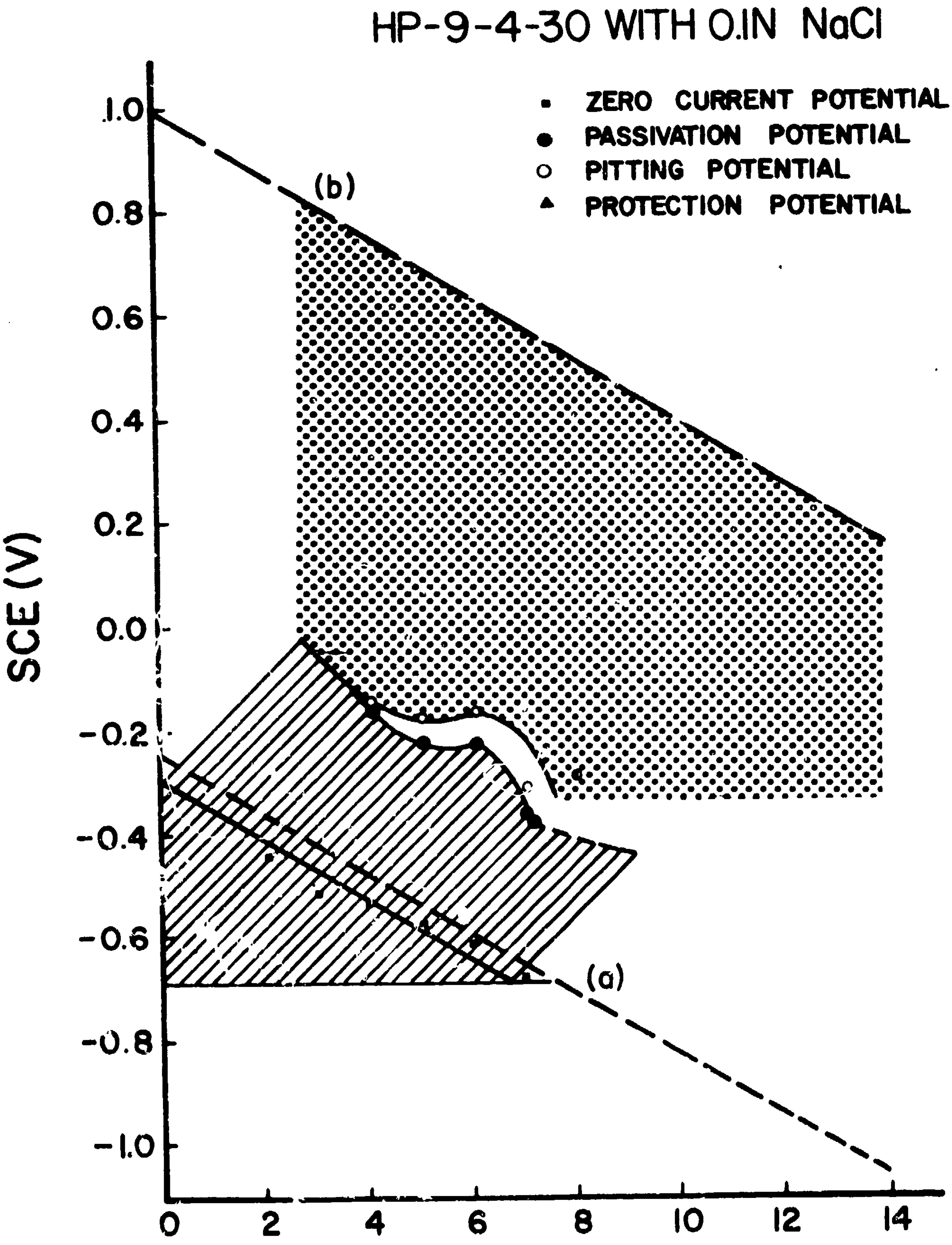
HP-9-4-30 WITH 0.1N NaCl
ZERO CURRENT POTENTIAL
PASSIVATION POTENTIAL
PITTING POTENTIAL
PROTECTION POTENTIAL
(b)
(a)
SCE (V)
1.0
0.8
0.6
0.4
0.2
0.0
-0.2
-0.4
-0.6
-0.8
-1.0
0
2
4
6
8
10
12
14

Figure 22. Experimental potential versus pH diagram for alloy HY180 in 0.1 M NaCl solution. Many features of the diagram for HY180 are similar to 4340 although the active corrosion region is considerably more extensive for HY180.

HY 180 WITH 0.1 NaCl

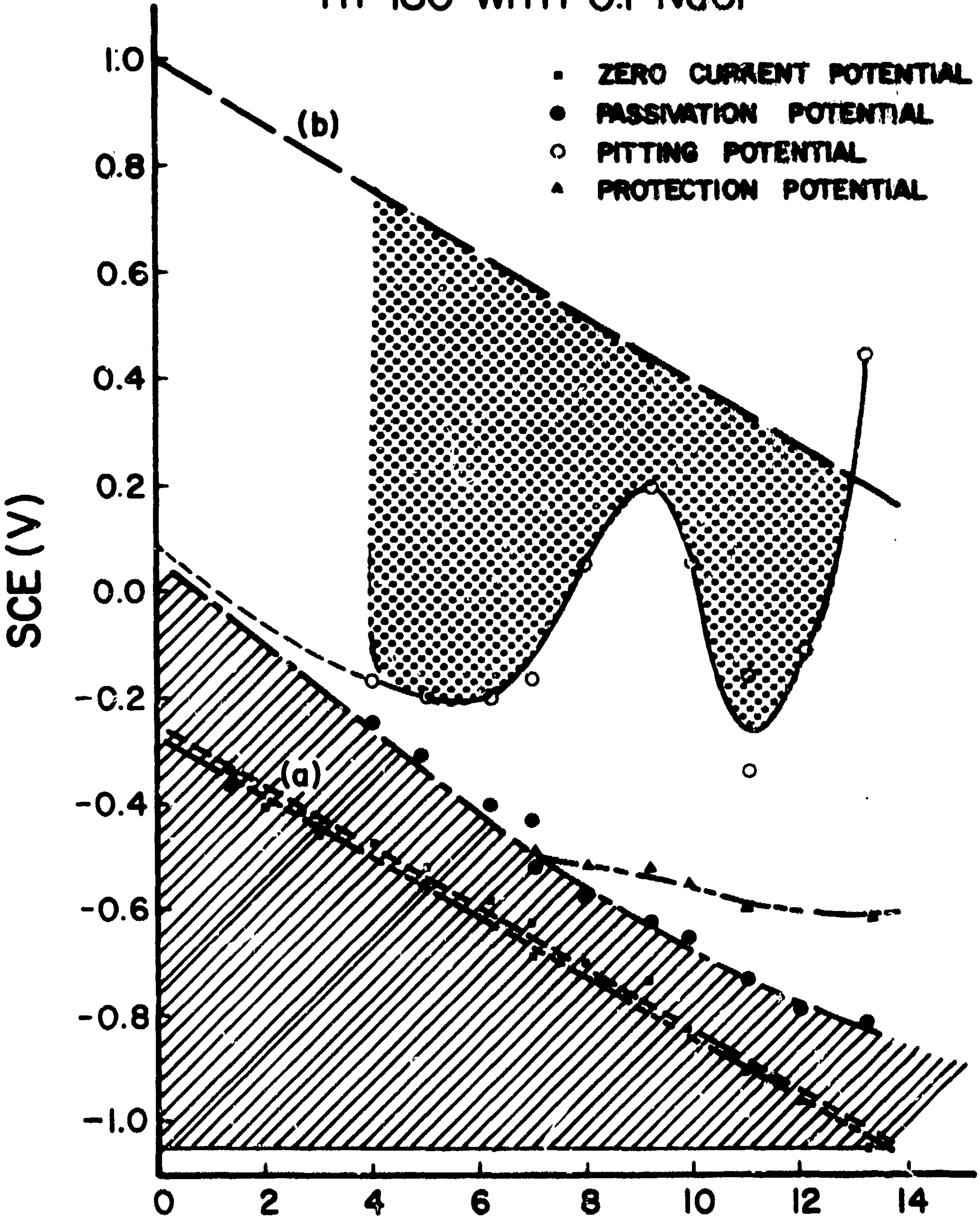

TABLE 10

CORROSION CURRENTS AT VARIOUS ELECTRODE POTENTIALS AS A FUNCTION OF PH

ALLOY 4340 IN 0.1 M NaCl

pH	Potential	Logarithm of Anodic Current Density (amps/cm^2)
	-0.500	-6
1.35	-0.490	-4
	-0.400	-2
	-0.500	-6
2.12	-0.495	-4
	-0.310	-2
	-0.525	-6
3.0	-0.510	-4
	-0.240	-2
	-0.580	-6
4.0	-0.550	-4
	-0.200	-2
	-0.600	-6
5.0	-0.570	-4
	0.0	-2
	-0.660	-6
6.22	-0.610	-4
	+0.060	-2
	-0.710	-6
6.8	-0.620	-4
	+0.060	-2
	-0.760	-6
8.08	-0.670	-4
	---	-2
	-0.640	-6
10.2	---	-4
	---	-2
	-0.190	-6
11.0	-0.130	-4
	-0.010	-2
	-0.220	-6
12.0	-0.190	-4
13.3	-0.700	-6

TABLE 11

CORROSION CURRENTS AT VARIOUS ELECTRODE POTENTIALS AS A FUNCTION OF PH

ALLOY 9-4-30 IN 0.1 M NaCl

pH	Potential	Logarithm of Anodic Current Density (amps/cm^2)
	-0.750	-6
10.0	---	-4
	---	-2
	-0.720	-6
9.0	---	-4
	---	-2
	-0.685	-6
8.5	---	-4
	---	-2
	-0.660	-6
8.0	---	-4
	---	-2
	-0.630	-6
7.0	---	-4
	---	-2
	-0.590	-6
6.0	-0.430	-4
	---	-2
	-0.520	-6
5.0	-0.420	-4
	---	-2
	-0.520	-6
4.0	-0.400	-4
	---	-2
	-0.520	-6
3.0	-0.480	-4
	0.0	-2
	-0.460	-6
2.0	-0.400	-4
	∿ +0.150	-2

TABLE 12

CORROSION CURRENTS AT VARIOUS ELECTRODE POTENTIALS AS A FUNCTION OF PH

ALLOY HY180 IN 0.1 M NaCl

pH	Potential	Logarithm of Anodic Current Density (amps/cm^2)
	-0.415	-6
2.0	-0.390	-4
	-0.110	-2
	-0.360	-6
1.35	-0.340	-4
	-0.180	-2
	-0.470	-6
4.0	-0.410	-4
	+0.080	-2
	-0.490	-6
5.0	-0.420	-4
	+0.050	∿ -2
	-0.600	-6
6.0	-0.520	-4
	+0.030	∿ -2
	-0.610	-6
7.0	-0.500	-4
	+0.100	-2
	-0.690	-6
8.3	-0.580	∿ -4
	+0.360	-2
	-0.730	-6
9.2	-0.620	∿ -4
	---	∿ -2
	-0.810	-6
9.9	---	-4
	---	-2
	-0.870	-6
11.1	-0.240	-4
	---	-2
	-0.960	∿ -6
12.0	-0.060	∿ -4
	---	-2
	-0.040	-6
13.0	+0.030	-4
	+0.640	-2

APPENDIX D

K_{Iscc} AND CRACK GROWTH RATE STUDIES

Compact tension specimens of 4340, 300M, 17-4 PH and HP 9-4-30 alloys, as shown in Figure 7, were used to determine the K_{Iscc} and crack growth rates in various enviroments. The specimen geometry corresponded with ASTM requirements (E399-70T, "Tentative Method of Test for Plane-Strain Fracture Toughness of Metallic Materials") for plane strain conditions. The stress intensity factor for such specimens can be obtained from the following equation:

$$K_I = P_I/(BW)^{1/2} \left[29.6(\frac{a}{w})^{1/2} - 185.5(\frac{a}{w})^{3/2} + 655.7(\frac{a}{w})^{5/2} - 1017.0(\frac{a}{w})^{7/2} + 638.9(\frac{a}{w})^{9/2}\right]$$

where P = candidate load, B = specimen thickness, W = specimen width, and a = crack length. The subscript "I" denotes candidate values of P and K which are subject to size ratio analysis. In order that the test specimens conform to plane-strain conditions, the ASTM method requires that both <u>B</u> and <u>a</u> satisfy the following size ratio criteria:

$$B \text{ and } a > \left(\frac{K_I}{T_{ys}}\right)^2$$

where T_{ys} = tensile yield strength. If these criteria are met, then K_I is a valid stress intensity value, K_{IC}, for the specimen.

A stressing frame incorporated in a creep machine, as shown in Figure 10, was used to laterally stress the specimens. Lateral stressing was used to facilitate the immersion of the specimens in a polyethylene or a plexiglass cell containing the test solution. The loading was accomplished by hydraulic actuators which provided a mechanical advantage of 1:200.

An EDI double cantilever displacement clip gage was used in conjunction with compliance curves to measure the crack length. The compliance curves were established by applying fixed loads and plotting the average crack length, a, as a function of the crack opening displacement (COD) as measured by the clip gage. The average crack length was obtained by measuring the crack length on both sides of the specimens.

Although the four alloys varied widely in their strength levels, all the specimens were initially fatigue precracked at 23 ksi$\sqrt{in}$. Tests in salt water solution only (no inhibitors added) showed that K_{Iscc} for 4340 and 300M specimens was below 23 ksi$\sqrt{in}$ whereas for HP 9-4-30 and 17-4 PH steels, a K of 23 ksi$\sqrt{in}$ was below their K_{Iscc} values. As such for all subsequent tests the 4340 and 300M specimens were further precracked to a K value of 10 ksi$\sqrt{in}$ (in decreasing steps, for example, from 23 to 18, 15, 12, 10 ksi$\sqrt{in}$) to obtain valid values of K_{Iscc} for these alloys.

The load (P) was incrementally applied to the specimens by carefully manipulating the hydraulic actuators starting at the K values as shown in Tables 7, 8 and 9. The magnitude of stepwise increments was 1 ksi$\sqrt{in}$. As shown by Raymond,[17] Figure 23, it is important to wait a significant amount of time before measuring K_{Iscc} values to assure that a fictitiously high K_{Iscc} value is not obtained. In the present study the specimens were stressed for period of several weeks in order to measure K_{Iscc}. The incubation time required for crack growth initiation may be a function of the alloy composition, as indicated in Figure 23. In addition, Figure 24[17] shows that the crack growth rate measurements are very sensitive to small modifications of environment and alloy microstructure (in this figure, lower hardness bainite versus higher hardness martensite). In the present study the effects of microstructure or alloy chemistry and environment on the incubation period and crack growth rate were clearly evident.

After failure of each specimen under overload conditions, the fracture surface was carefully inspected to be certain that cracking had proceeded uniformly across the specimen thickness and that the crack front had suffered minimum amount of curvature.

The determination of K_{Iscc} and (da/dt) for these alloys in this manner provides a quantitative means of measuring the susceptibility to stress corrosion cracking of the alloys in various aqueous environments, and can indicate the effectiveness of chemical inhibitor additions to the bulk (NaCl) solution in preventing or retarding crack propagation at loads less than the critical stress intensity, K_{IC}.

Data showing K_{Iscc} and crack growth characteristics of the various test alloys are included as Figures 25-29 inclusive. The results are summarized in Tables 7, 8 and 9.

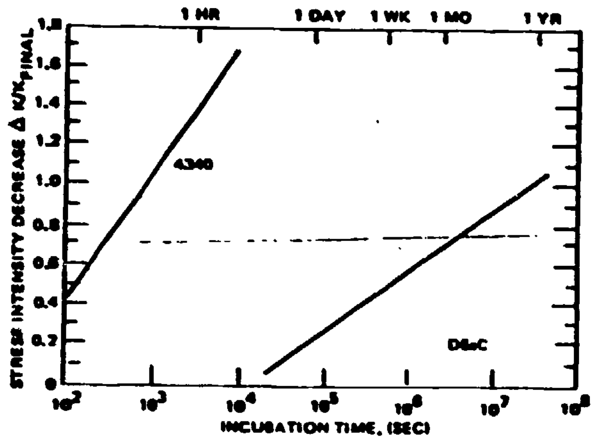

Figure 23. Stress History Effect in Stress-Corrosion Cracking.

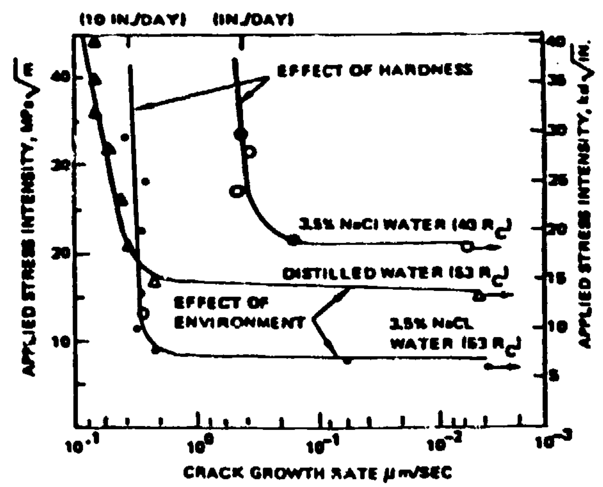

Figure 24. Factors that Affect the Crack Growth Rate of High-Strength AISI 4340 Steels in Aqueous Environments.

Figure 25. Crack Growth Rate versus Stress Intensity for alloy 4340 exposed to various environments.

Exposures: Specimen C4-25 uninhibited 0.1 M NaCl solution.

Specimen C4-26 .01X Nalco 39L in 0.1 M NaCl solution.

Specimen C4-33 1X Nalco 39L in 0.1 M NaCl solution.

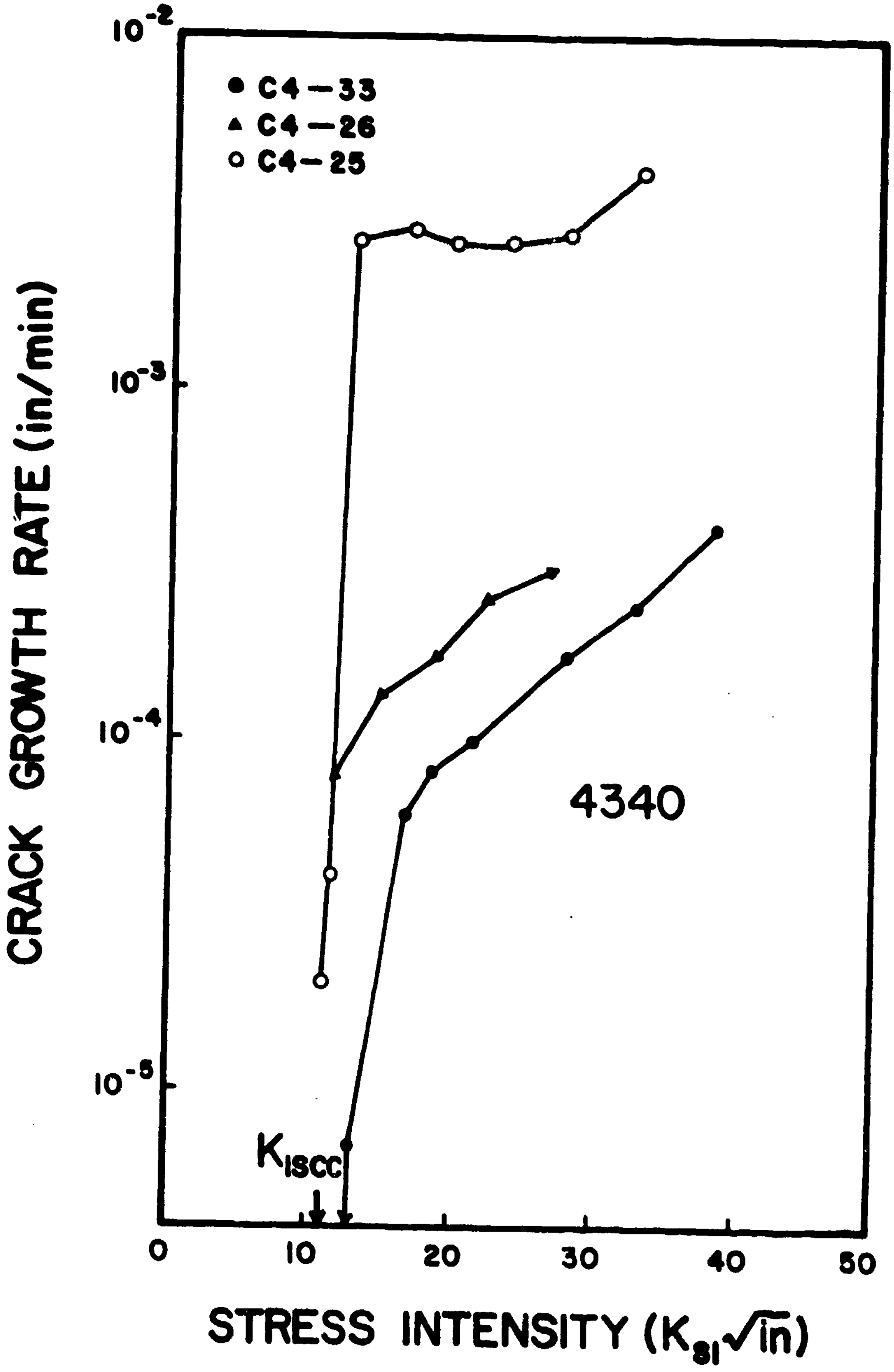
10^-2
10^-3
10^-4
10^-5
● C4—33
▲ C4—26
○ C4—25
4340
K ISCC
0
10
20
30
40
50
CRACK GROWTH RATE (in/min)
STRESS INTENSITY (KSI√in)

Figure 26. Crack Growth Rate versus Stress Intensity for alloy 4340 exposed to various environments.

Exposures: Specimen C4-27 0.01 M piperazine in 0.1 M NaCl solution.

Specimen C4-28 0.01 M piperidine in 0.1 M NaCl solution.

Specimen C4-34 1.0 M piperazine in 0.1 M NaCl solution.

1.0 M piperazine increased K_{Iscc} from $\sim$10 for uninhibited solution, Figure 25, to 61 for alloy 4340 with $\sigma_{YS} \simeq 265$ ksi.

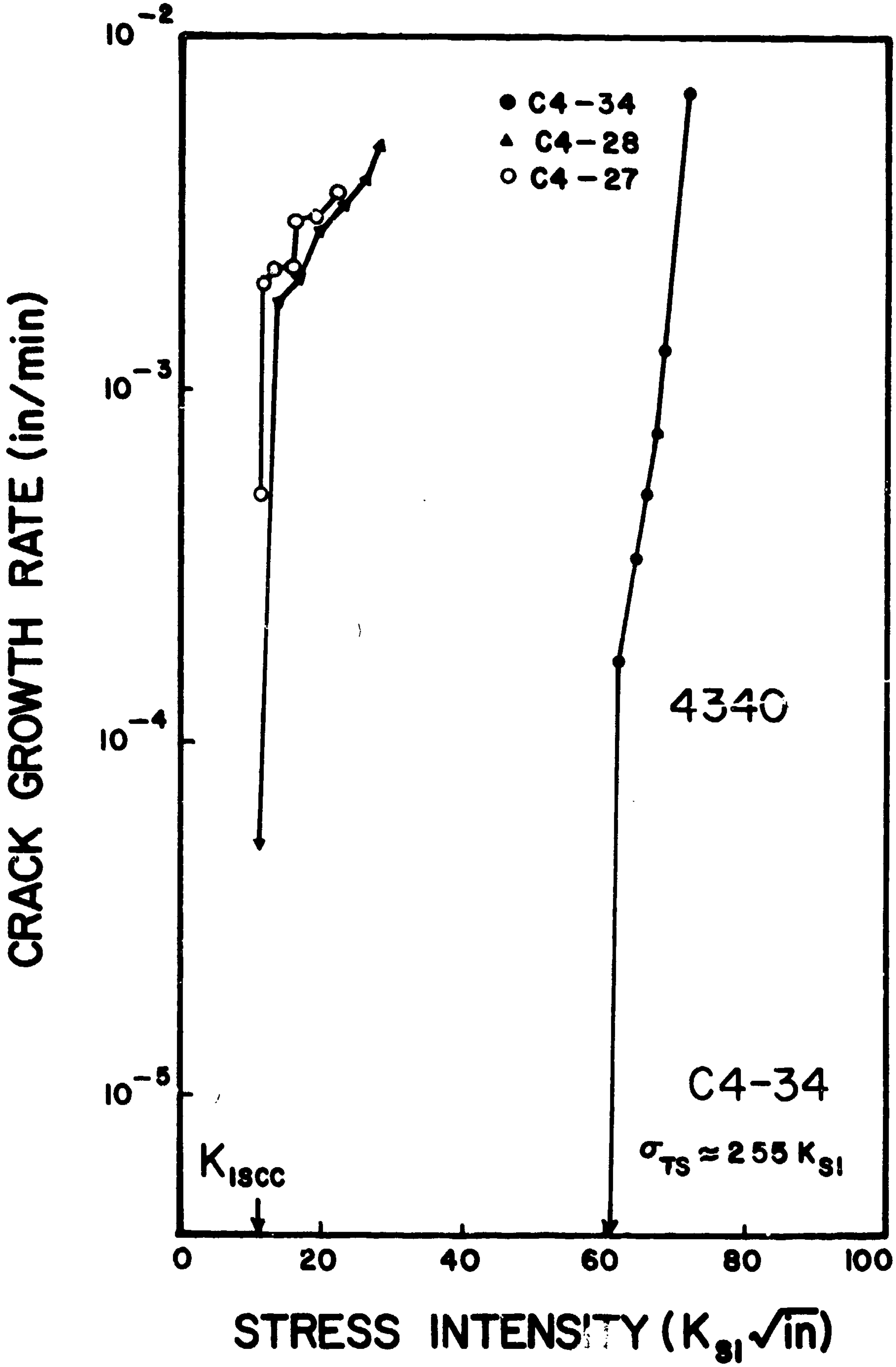

CRACK GROWTH RATE (in/min)
10^{-2}
10^{-3}
10^{-4}
10^{-5}
● C4-34
▲ C4-28
○ C4-27
4340
C4-34
$\sigma_{TS} \approx 255\ K_{SI}$
K_{ISCC}
0
20
40
60
80
100
STRESS INTENSITY ($K_{SI}\sqrt{in}$)

Figure 27. Crack Growth Rate versus Stress Intensity for alloy 300M exposed to various environments.

Exposure: Specimen C3-12 uninhibited 0.1 M NaCl solution.

Specimen C3-13 0.01X Nalco 39L in 0.1 M NaCl solution.

Specimen C3-15 0.1X Nalco 39L in 0.1 M NaCl solution.

Specimen C3-10 1.0 M piperidine in 0.1 M NaCl solution.

Speicmen C3-11 1.0 M piperazine in 0.1 M NaCl solution.

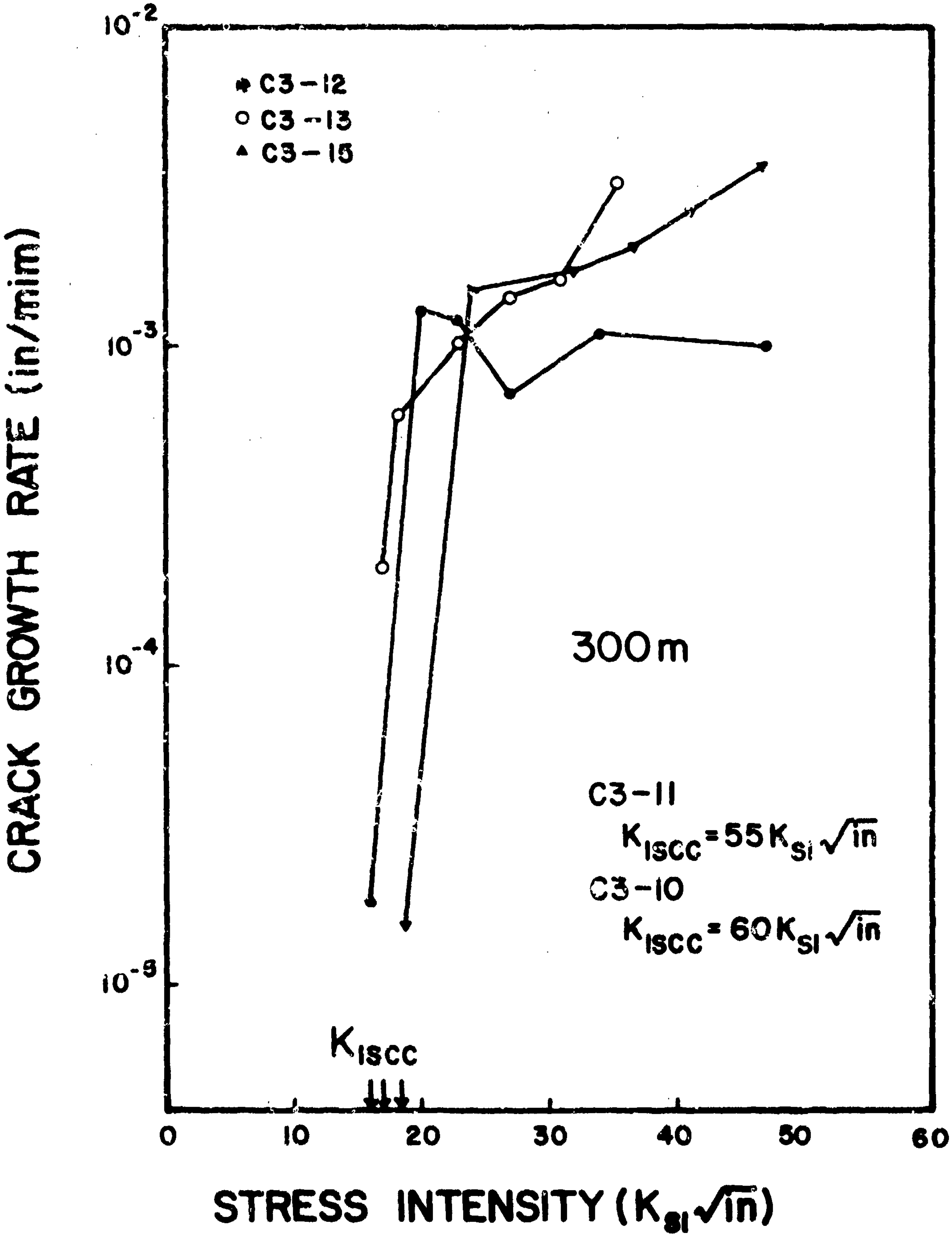

CRACK GROWTH RATE (in/mim)
10^-2
10^-3
10^-4
10^-5
C3-12
C3-13
C3-15
300m
C3-11
K ISCC = 55 K SI √in
C3-10
K ISCC = 60 K SI √in
K ISCC
0
10
20
30
40
50
60
STRESS INTENSITY (K SI √in)

Figure 28. Crack Growth Rate versus Stress Intensity for alloy 17-4 PH exposed to various environments.

Exposures: Specimen C1-12 uninhibited 0.1 M NaCl solution.

Specimen C1-13 0.1X Nalco 39L in 0.1 M NaCl solution.

Specimen C1-14 1.0 M piperazine in 0.1 M NaCl solution.

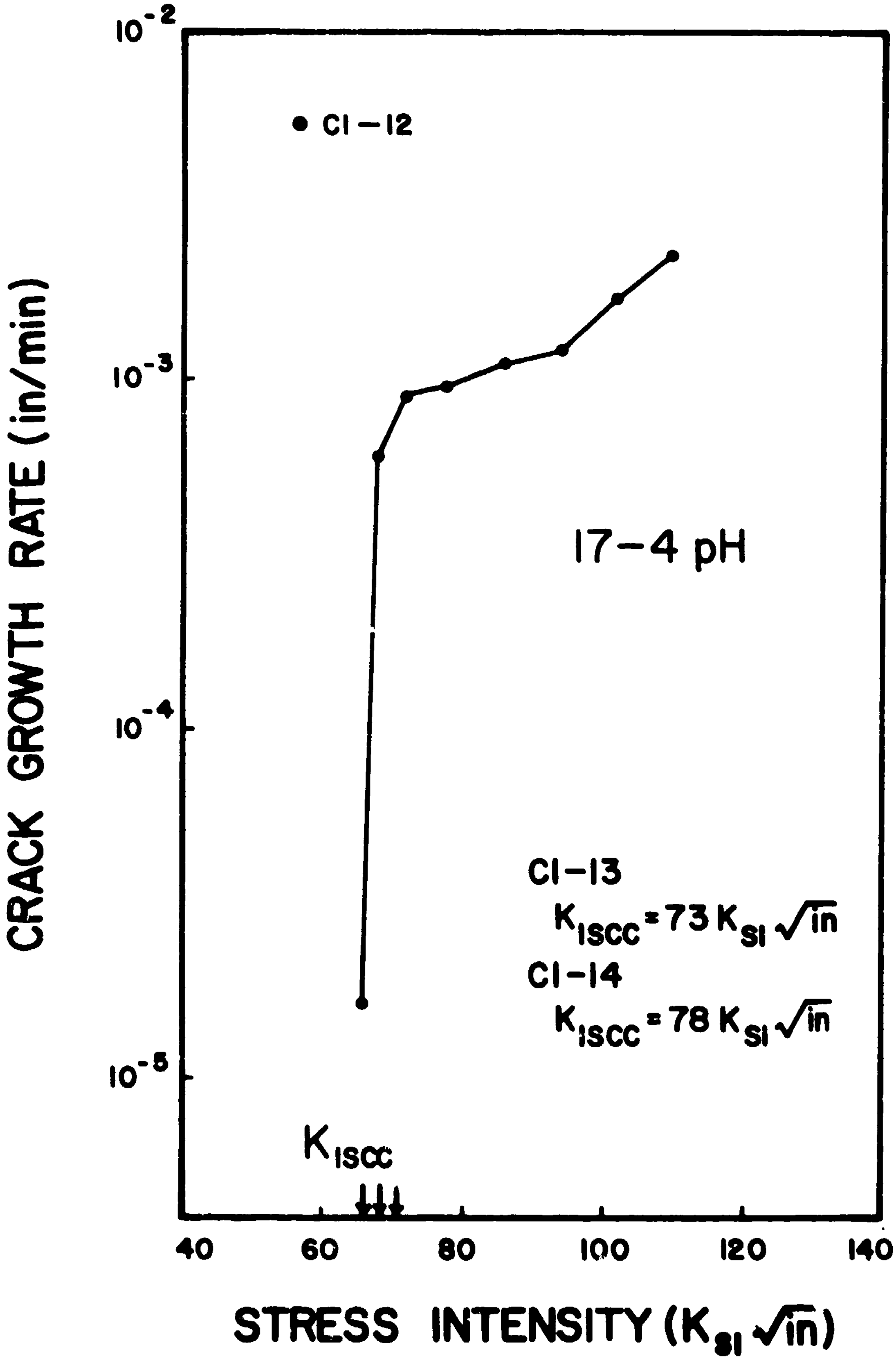

CRACK GROWTH RATE (in/min)
10^-2
10^-3
10^-4
10^-5
• CI-12
17-4 pH
CI-13
K_ISCC = 73 K_SI √in
CI-14
K_ISCC = 78 K_SI √in
K_ISCC
40
60
80
100
120
140
STRESS INTENSITY (K_SI √in)

Figure 29. Crack Growth Rate versus Stress Intensity for alloy HP 9-4-30 exposed to various environments.

Exposures: Specimen CH-6 uninhibited 0.1 M NaCl solution.

Specimen CH-7 1X Nalco 39L in 0.1 M NaCl solution.

Specimen CH-8 1.0 M piperazine in 0.1 M NaCl solution.

Specimen CH-9 1.0 M piperidine in 0.1 M NaCl solution.

All three inhibitors increased K_{Iscc} and reduced crack growth rate significantly as compared with uninhibited chloride solution.

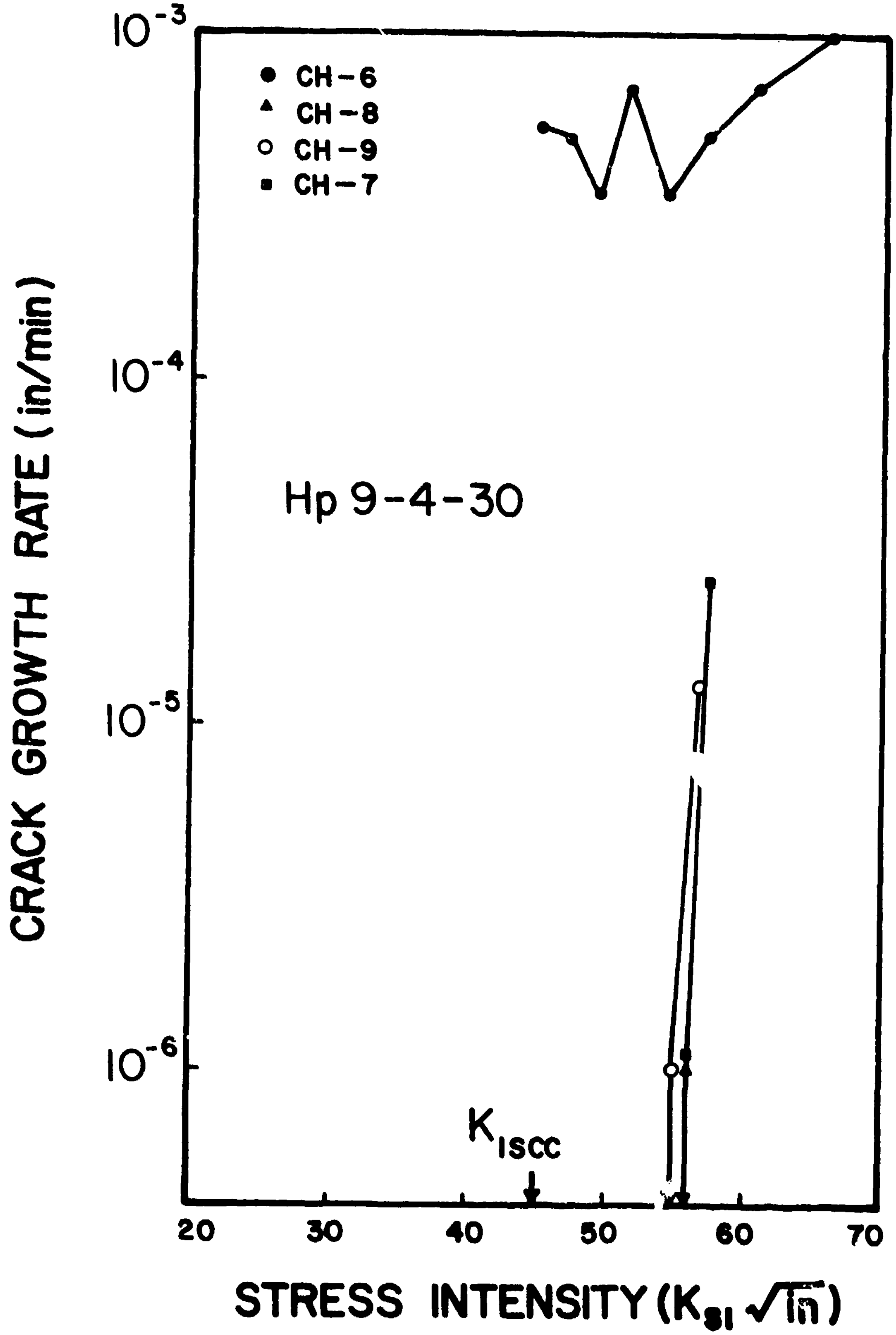

*U.S.Government Printing Office: 1979 — 657-002/449